

Fall 12-20-2018

Geomorphology of shell ridges and their effect on the stabilization of the Biloxi Marsh, East Louisiana

Frances R. Crawford
University of New Orleans, frcrawfo@uno.edu

Follow this and additional works at: <https://scholarworks.uno.edu/td>



Part of the [Geology Commons](#), [Geomorphology Commons](#), and the [Stratigraphy Commons](#)

Recommended Citation

Crawford, Frances R., "Geomorphology of shell ridges and their effect on the stabilization of the Biloxi Marsh, East Louisiana" (2018). *University of New Orleans Theses and Dissertations*. 2544.
<https://scholarworks.uno.edu/td/2544>

This Thesis is protected by copyright and/or related rights. It has been brought to you by ScholarWorks@UNO with permission from the rights-holder(s). You are free to use this Thesis in any way that is permitted by the copyright and related rights legislation that applies to your use. For other uses you need to obtain permission from the rights-holder(s) directly, unless additional rights are indicated by a Creative Commons license in the record and/or on the work itself.

This Thesis has been accepted for inclusion in University of New Orleans Theses and Dissertations by an authorized administrator of ScholarWorks@UNO. For more information, please contact scholarworks@uno.edu.

Geomorphology of shell ridges and their effect on the stabilization of the Biloxi
Marsh, East Louisiana

A Thesis

Submitted to the Graduate Faculty of the
University of New Orleans
in partial fulfillment of the
requirements for the degree of

Master of Science
In
Earth and Environmental Sciences
Coastal and Geomorphic Studies

by

Frances Crawford

B.S. Louisiana State University, 2016

December, 2018

Copyright 2018, Frances Crawford

Acknowledgements

I, first and foremost, would like to thank my advisor, Dr. Mark Kulp. His guidance throughout this project has been incredibly appreciated and his help in teaching me how to become a better scientist was invaluable. Secondly, my committee members, Dr. Ioannis Georgiou and Dr. Carol Wilson, were both critical in offering great advice and a fresh perspective on the project.

In addition, I had amazing support from students and staff at UNO including Mike Brown, Joseph Hankerson, Liz Larroux, Jared Bullock, and Tara Yocum. A special thanks goes to Julie Torres and Jarrett Levesh, not just for help in the field, but also in staying sane throughout classes and thesis work. I am also extremely grateful to Ben Beasley and Celeste Woock for always having the answers to my ArcGIS questions and allowing for countless conversations to vent. Furthermore, I received great help from Dr. Michael Poirrier and Dr. Tom Soniat in identifying shell species. As a geologist, that particular task was not my greatest strength.

It is also imperative that I thank my family and friends outside of UNO who have provided support in numerous ways outside of academia: my mom, Kathy Crawford; my dad, Charlie Crawford; my cousin, Carmen Carlos; and my friends, Megan Altemus and Patricia Sheridan.

Table of Contents

List of Figures	vi
List of Tables	vii
Abstract	viii
CHAPTER 1. INTRODUCTION	1
1.1 Pontchartrain Basin	1
1.2 Biloxi Marsh.....	3
1.2.1 Shell ridges in the Biloxi Marsh.....	5
1.2.1.1 <i>Shell ridges vs. shell cheniers</i>	7
1.3 Study Objectives	10
CHAPTER 2. METHODS	11
2.1 Marsh Island and Shell Ridge Selection	11
2.2 Shell Ridge Translation, Area, and Volume Measurements	12
2.3 Shell Analysis.....	14
2.4 Grab Samples	14
2.5 Marsh Biomass Analysis.....	15
2.6 Aerial and Satellite Imagery for Geomorphic History	16
CHAPTER 3. RESULTS.....	17
3.1 Shell Ridge Translation, Area, and Volume Measurements	17
3.2 Shell Analysis.....	21
3.3 Grab Samples	24
3.4 Marsh Analysis.....	25
3.4.1 Aboveground biomass	25
3.4.1.1 <i>Sites without a ridge</i>	25
3.4.1.2 <i>Sites with a stable ridge</i>	26
3.4.1.3 <i>Sites with a mobile ridge</i>	26
3.4.2 Belowground biomass	27
3.4.2.1 <i>Sites without a ridge</i>	27
3.4.2.2 <i>Sites with a stable ridge</i>	27
3.4.2.3 <i>Sites with a mobile ridge</i>	27
3.4.3 Data analysis.....	29
3.5 Aerial and Satellite Imagery.....	29
CHAPTER 4. DISCUSSION	33
4.1 Shell species, origin, and marsh-edge accumulation.....	33
4.2 Shell ridge movement.....	37

4.2.1 Effect of storm surge and wind direction	37
4.2.2 Effect of individual ridge characteristics, fetch conditions, and wind direction	37
4.3 Shell ridge effect on marsh.....	39
4.3.1 Future work.....	42
4.4 Future of Biloxi Marsh due to shell presence	42
CHAPTER 5. CONCLUSION.....	44
References.....	46
Appendix.....	50
Vita.....	52

List of Figures

Figure 1.....	2
Figure 2.....	4
Figure 3.....	5
Figure 4.....	6
Figure 5.....	8
Figure 6.....	9
Figure 7.....	11
Figure 8.....	18
Figure 9.....	19
Figure 10.....	20
Figure 11.....	22
Figure 12.....	22
Figure 13.....	23
Figure 14.....	25
Figure 15.....	28
Figure 16.....	30
Figure 17.....	31
Figure 18.....	34
Figure 19.....	36
Figure 20.....	41

List of Tables

Table 1.....	50
Table 2.....	50
Table 3.....	51
Table 4.....	24
Table 5.....	31

Abstract

Extensive shell ridges frame the edges of marsh platforms in parts of the Biloxi Marsh of southeast Louisiana. The exact sources of the shells in these accumulations have not been clearly identified but the most likely source is a combination of shells from modern offshore and shells excavated from buried St. Bernard delta deposits. Larger or fetch-protected ridges remain stable through time, whereas ridges facing open water are more mobile, moving as much as 38 m inland from July 2017 to January 2018. Behind stable ridges, marsh platform biomass is relatively unaffected. When ridges are mobile, vegetation is smothered, leaving an exposed platform that lacks aboveground vegetation to dampen wave energy and fragments into “blocks” along its terraced edge, which in turn are deposited onshore. In the future, marshes will likely erode fastest in areas where shell ridges are mobile and remain resistant where shell ridges are stable.

Keywords: shell ridges, marsh edge erosion

CHAPTER 1. INTRODUCTION

Louisiana coastal marshes are a rapidly disappearing environment and constitute a last defense for mainland communities from the threats of sea level rise and tropical cyclone storm surges (Gedan et al., 2011). Between 1932 and 2010, Louisiana wetland losses totaled 25% or 4,877 km² (Couvillion et al., 2011). Natural processes such as sea-level rise, subsidence, and storm surges, combined with human modifications to the wetlands in the form of levees and canals, have been suggested to be contributors to the coast-wide land loss (Kesel, 1988; Day and Templet, 1989; Day et al., 2000; Törnqvist, 2008; Mariotti et al., 2010; Meade and Moody, 2010).

The geomorphic styles and processes of wetland loss vary across the coast (Penland et al., 2002) and observations of coastal wetland loss reveal that not all wetlands are subject to the exact same processes of wetland loss. This study focuses on a previously undocumented process of wetland loss in the Biloxi Marshes of the Pontchartrain Basin, which field and imagery observations suggest is widespread across the shell-rich marsh of eastern coastal Louisiana (Fig. 1).

1.1 Pontchartrain Basin

The Pontchartrain Basin is a hydrologic basin that extends across the north-east portion of the Louisiana coastal zone. Couvillion et al. (2011) reported that the Pontchartrain Basin lost 503 km² from 1932 to 2010 (~18% of initial area), whereas Fearnley et al. (2009) reported a total land loss of 871 km² during two periods, from 1932-1990 and 1990-2001, with annual rates for those time periods at 13 km² and 12 km² respectively. Differences in total land loss reported by Couvillion et al. (2011) compared to Fearnley et al. (2009) are an outcome of the slightly

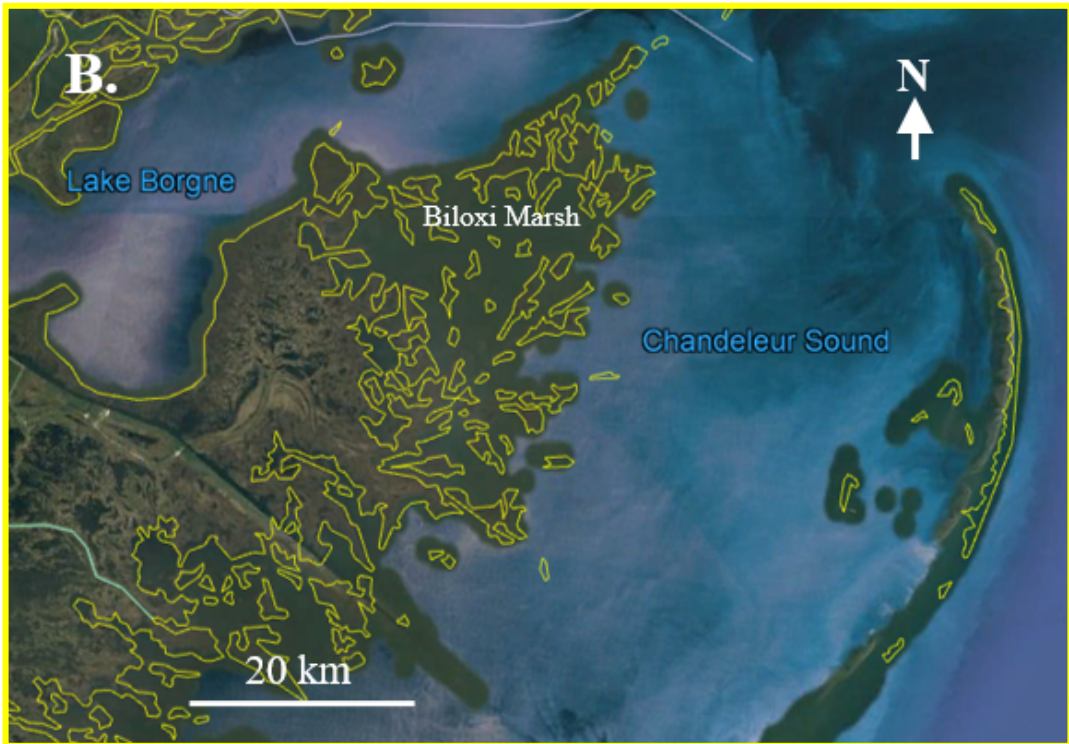
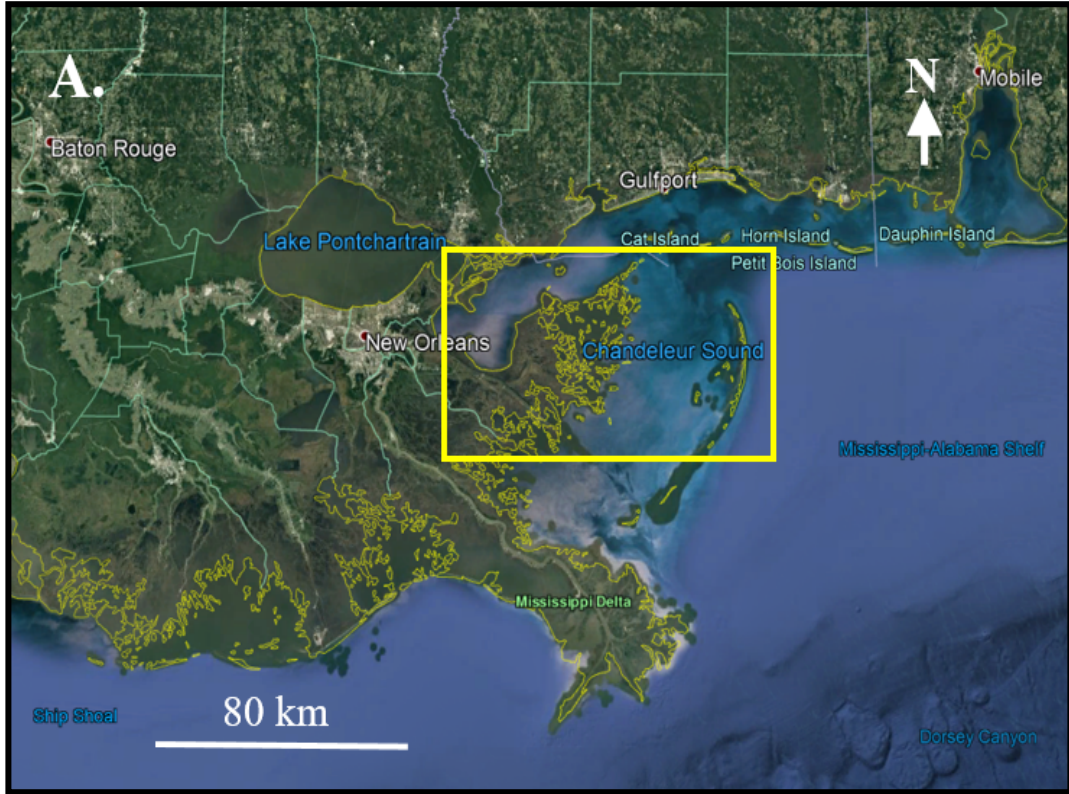


Figure 1: (A) Base map showing the location of Biloxi Marsh, east of New Orleans. (B) Location of Little Bayou Pierre (red box) in Biloxi Marsh, which is framed by Lake Borgne and the Chandeaur Sound (2016 imagery from *Google Earth*).

different geographic domains of the Pontchartrain Basin that each effort used.

Couvillion et al. (2011) provided no discussion to causes of land loss, but Fearnley et al. (2009) primarily attributed wetland loss in the Basin to direct removal of land by man-made actions and submergence in the 1932-1990 time frame and to primarily shoreline erosion from 1990-2001. Processes of wetland loss are not uniform across the Pontchartrain Basin and locally a process of wetland loss could be dominate yet not be fully documented. One process of wetland loss that appears to be a significant factor within the Biloxi Marsh of the eastern Pontchartrain Basin appears to be related to the widespread accumulation of shells on the marsh edges (Fig. 2), which appear to be contributing to vegetative dieback and ultimately enhanced marsh edge erosion.

1.2 Biloxi Marsh

The Biloxi Marsh (Fig. 1) represents a portion of the land constructed from the Holocene Mississippi River Delta system (Fig. 3). Processes of fluvial progradation, avulsion, and ultimately marine transgression collectively created the fluvial, deltaic, and marine landscape of southern Louisiana (e.g. Fisk, 1955; Roberts, 1997). The Biloxi Marsh specifically is a result of fluvial progradation associated with the St. Bernard delta complex, which became active approximately 3.5 ka. (Törnqvist, 1996) as distributaries prograded across the eastern Louisiana continental shelf. Core and shallow seismic data indicate that distributaries of the St. Bernard delta complex prograded towards the northeastern Louisiana shelf, then advanced east beyond the present location of the Chandeleur Islands (Kindinger, 1988; Rodgers, 2009). At approximately 1.4 ka abandonment of the delta complex began (Törnqvist, 1996) and processes such as marine working and relative sea level rise modified the landscape to create the modern geomorphology of the Biloxi Marsh (Penland et al., 1988; Roberts, 1997).

Today, the Biloxi Marsh is framed by Lake Borgne to the west and Chandeleur Sound to the east (Fig.1). Its marsh platforms are dominantly vegetated by *Spartina alterniflora* and with sand-rich shorelines absent throughout, the primary allochthonous sediment fringing the marsh



Figure 2: Photographs of shell ridges in the Biloxi Marsh discussed in this study. Upper picture is of Ridge 7 on 6/9/17 (height ~0.72 m measured on 7/26/17) and the lower picture taken on 9/13/17 is of Ridge 6 (height 1.26 m measured on 9/13/17).

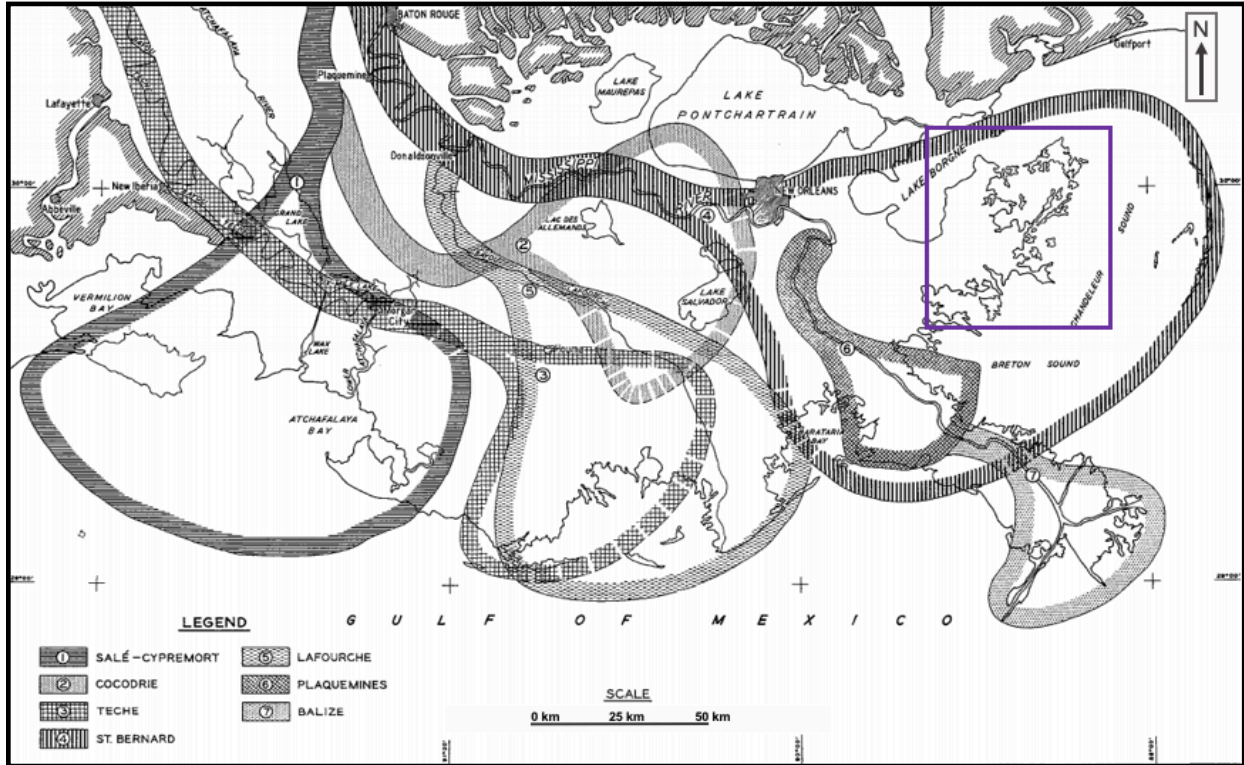


Figure 3: Holocene delta lobes of the Mississippi River that began prograding at approximately 8.0 Ka. Note the location of the St. Bernard lobe and the location of the Biloxi Marsh (purple box) within the area covered by the St. Bernard lobe (from Kolb and van Lopik, 1958).

consists of whole and fragmented shells, primarily *Crassostrea virginica* (Ellison, 2011). The scarped marsh edges in this area are often terraced, a feature studied by Thomason (2016) and Trosclair (2013), and are the result of wave action during low water conditions (Tonelli et al. 2010; Trosclair, 2013).

1.2.1 Shell ridges in the Biloxi Marsh

Across the Biloxi Marsh, numerous shell accumulations exist as marsh-edge parallel ridges (Fig. 2). Ellison (2011) suggested that the abundance of these shell ridges is a result of limited sand-rich strata in the subsurface of the Biloxi Marsh (Ellison, 2011) and the hydrodynamic properties of shells and shell fragments. The drag coefficient, which is almost independent of the Reynolds number, increases with particle surface roughness and particle elongation (Allen, 1984). In addition, large lift surfaces, low settling velocity, and large

resistance to flow friction of whole and fragmented shell enables easier sorting from siliclastic sand, the ability during flooding conditions to be carried by swash and current processes, and, if imbricated as a sedimentary unit, a resistance to re-suspension (Weill et al., 2010).

The formation of these shell ridges has been suggested to be a result of high-energy events that transport shells onto the marsh platform where they are deposited in ridge to mound-like accumulations stratigraphically above marsh platform biomass and mud (Ellison, 2011). A

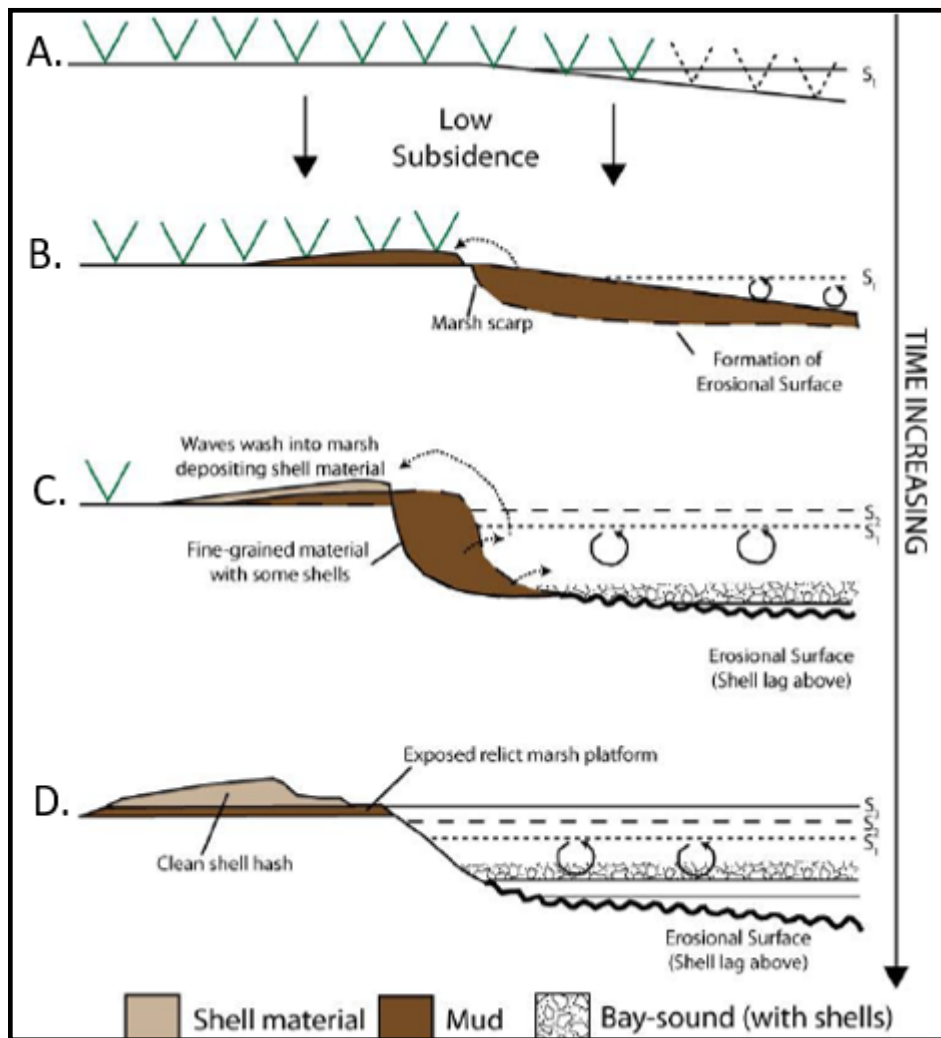


Figure 4: Geomorphic process of shell berms formation. Phases A-B illustrate the erosion of the marsh that leads to the creation of a scarp (Wilson and Allison, 2008). The then suspended sediments are ultimately washed onshore by wave and tidal action. Eventually, storm events lead to the erosion and suspension of bay-bottom deposits that then deposit shell material onshore. Stages C & D illustrate how when the marsh is covered in shells, it both protects the marsh and prevents accretion (Ellison, 2011).

suite of mechanisms and conditions required for the formation of these shell ridges (Fig. 4) was suggested by Ellison (2011) on the basis of a Wilson and Allison (2008) conceptual model that describes marsh-edge erosion. The model initiates with Stages A and B directly from Wilson and Allison (2008), however, Ellison (2011) describes Stage B differently. Ellison (2011) begins with Stage A, a subsiding marsh, whereas Stage B continues with the formation of a scarp on the marsh edge. Sediment liberated by the erosion of the marsh edge and other available sediment is transported onshore by wave and tidal action, and eventually during extreme events (ex: tropical storms, cold fronts) shells are eroded from bay-bottom strata and deposited onshore as well. Stages C and D illustrate how when the marsh is covered in shells, it both protects the marsh and prevents accretion (Fig. 4).

1.2.1.1 Shell ridges vs. shell cheniers

The stratigraphy and suggested mode of formation for the marsh platform shell ridges differentiate these ridges from another common type of shell accumulation, the shell chenier (Fig. 5). The term chenier was first introduced by Russell and Howe (1935) referring to the oaks (French: *chêne*), which often grow along the elevated ridges and mounds of southwest Louisiana. Cheniers are well studied along southwest Louisiana (Russell and Howe, 1935; Byrne, 1959; Gould and McFarlan, 1959; Hoyt, 1969; Otvos and Price, 1979) and other locations such as East China (Cangzi and Walker, 1989), southeast England (Neal et al., 2002), Suriname (Augustinus, 1980), and Spain, (Rodríguez-Ramírez and Yáñez-Camacho).

Cheniers have a multitude of definitions based on their formation and evolution (Rhodes, 1980). In this study, cheniers are recognized as relict features (*sensu* Otvos, 2000) that developed in response to fluctuations in sediment abundance and deficit. For example, along the southwest Louisiana chenier plain, the coast-parallel sand and shell ridges separated by mud-rich

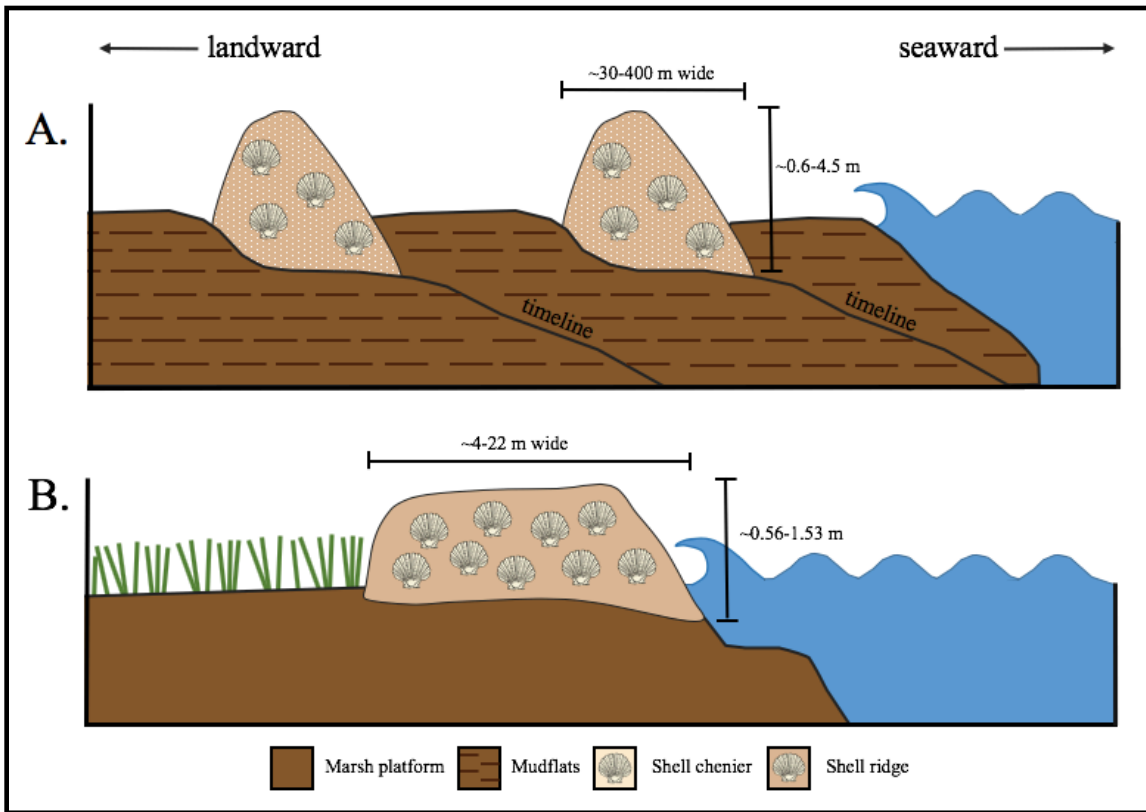


Figure 5: Illustration comparing the stratigraphy of shell cheniers and shell ridges. (A) Chenier stratigraphy of alternating mudflats facies and shell cheniers. Note how shell cheniers are rooted in the subsurface. Chenier stratigraphy is developed from alternating periods of high and low sediment input and marine reworking. For example, when riverine sediment is high, mudflats develop, then when riverine sediment input is low, the existing sediment is reworked leading to a sediment winnowing and concentration of larger clasts (sand and shell deposits). (B) Shell ridge stratigraphy of ridge stratigraphically situated above marsh platform edge, deposited by strong wave action from storms.

troughs are the result of periods of high riverine sediment flux when mudflat progradation takes place followed by periods of diminished sediment input (Otvos and Price, 1979; Reineck and Singh, 1980). During reduced sediment input, previously deposited material is reworked, leading to sediment winnowing and concentration of shell-rich deposits along the shore, a process that can be repeated many times (Otvos and Price, 1979; Reineck and Singh, 1980). Chenier width around the world commonly varies from 30-400 m (Hoyt, 1969; Otvos and Price, 1979; Rhodes, 1980; Liu and Walker, 1989) and cheniers of southwestern Louisiana are described as often stratigraphically rooted to the subsurface (Otvos and Price, 1979; see Fig. 5). The physical and stratigraphic differences between the classic cheniers of western Louisiana (with similar

counterparts in East China and Suriname) and those of the Biloxi Marsh, require a more appropriate term for the latter, and herein they are referred to as *active shell ridges*. At least one other example of active shell ridges exists along the Georgia coast (Alexander, 2008). The stratigraphy of the Biloxi marsh shell ridges, like active shell ridges, is also a single geomorphic feature of shell material that simply sits directly on the edge of a marsh platform, instead of developing from alternating periods of mudflat progradation and sediment winnowing.

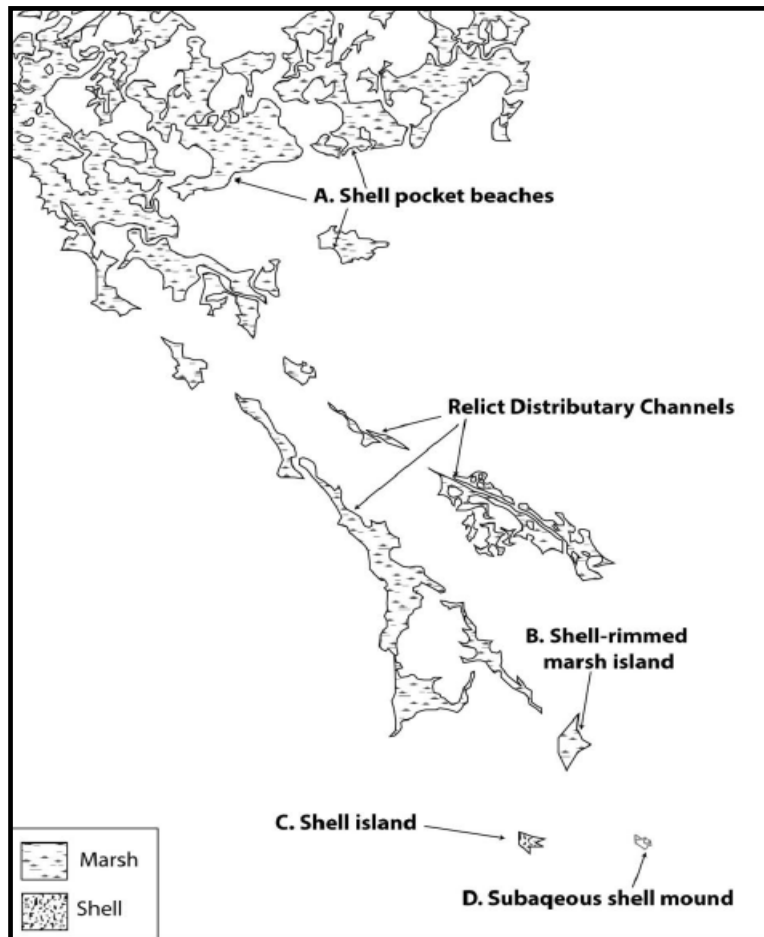


Figure 6: Map of a portion of the Biloxi marsh landscape with common morphological features such as relict distributary channels, a shell-rimmed marsh island, a shell island, and a subaqueous shell mound. These geomorphic features suggest an evolutionary sequence wherein, shell pocket beaches, through erosion and relative sea level rise, can evolve into shell-rimmed marsh islands, and eventually subaqueous shell mounds (Ellison, 2011).

Ellison (2011) suggested that the accumulation of shells in the Biloxi marsh initially forms shell-paved pocket beaches, and that fragmentation of the marshes eventually leads to

isolated shell-rimmed marsh islands. Ellison (2011) provided no real mechanism for the fragmentation but Reed (1989a) attributed the formation of Louisiana marsh islands to ponding and bay expansion. Ellison (2011) does explain that the presence of the isolated shell-rimmed marsh islands is due to underlying resistant landmasses that form good foundations, such as natural levee and point bar deposits, a concept noted by Kolb and van Lopik (1958). These marsh islands eventually succumb to relative sea level rise, resulting in subaqueous shell mounds (Ellison, 2011; see Fig. 6).

A study by Thomason (2016) focused on marsh-edge erosion in the Biloxi Marsh and examined two active shell ridges, which she simply called shell berms. These ridges translated inward onto the marsh as much as 12 m during a period of 34 days. This movement was attributed to the wind-driven waves with water set-up created during extratropical cyclones.

1.3 Study Objectives

An array of mechanisms that can lead to wetland loss have been identified for coastal Louisiana marshes, yet the effect of active shell ridges on marsh platforms has not been evaluated. There is no study that fully documents the source of the shells or that explains the impact of these ridges on marsh platforms.

The objectives of this study are to: 1) identify the shellfish species contributing to the shell accumulations as well as their source, 2) document shell ridge morphologic evolution and the mechanisms that exert a control on ridge movement (e.g. storm activity, or wave and tide energy), 3) evaluate the impact of the shell ridges to the marsh, and 4) predict how the marsh islands will look in the future due to shell ridge presence.

CHAPTER 2. METHODS

2.1 Marsh Island and Shell Ridge Selection

Using satellite imagery from the Biloxi Marsh, locations with shell-rich accumulations were identified. In the satellite imagery, shell ridges show as very bright white features that parallel the marsh edges. On the basis of this visual assessment, “Little Bayou Pierre” appeared to have some of the most laterally persistent marsh-edge shell ridges (Fig. 7), which was confirmed shortly thereafter by a site visit.

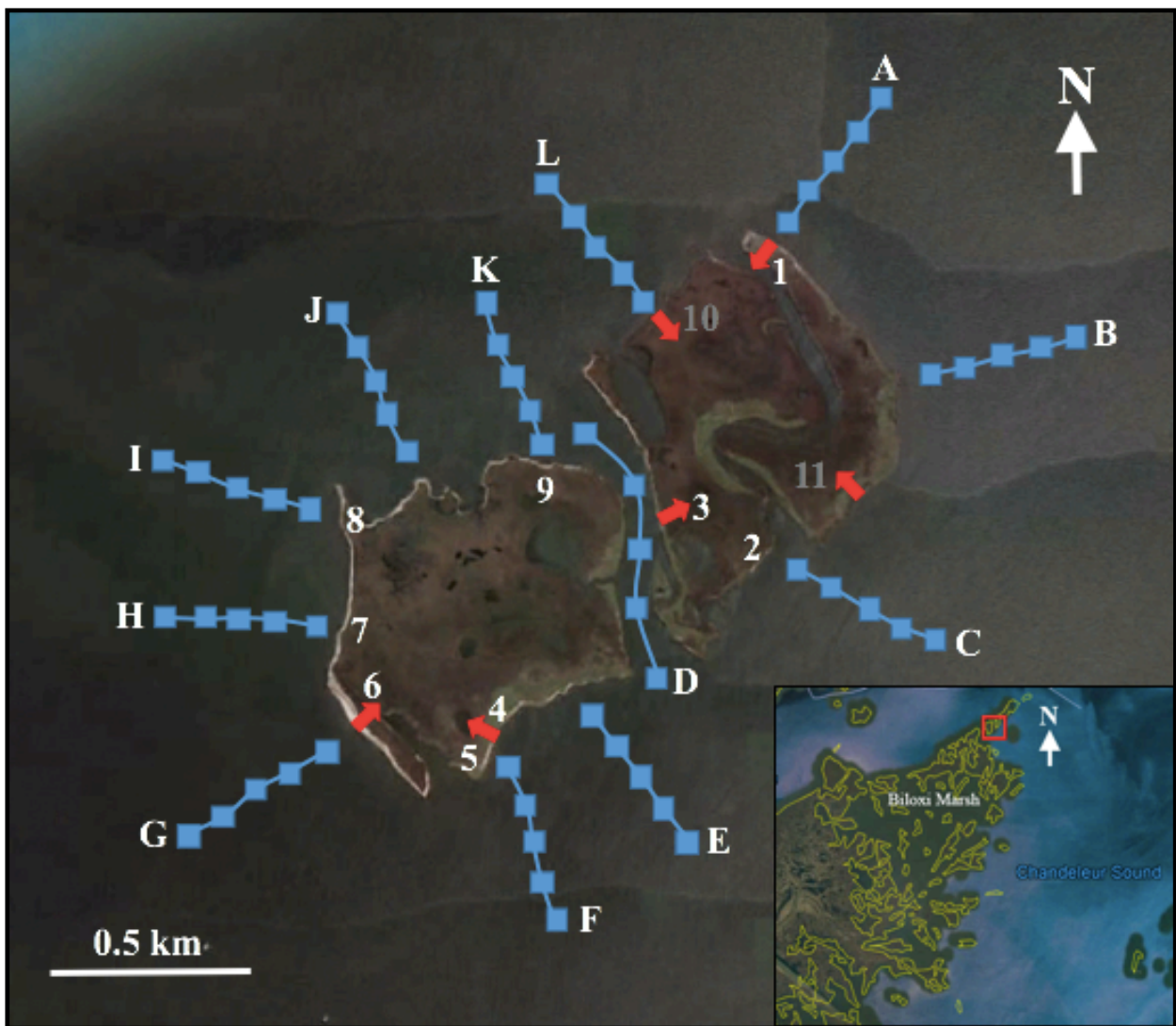


Figure 7: Base map of the shell-rimmed marsh island study site known as Little Bayou Pierre. Map shows shell ridge study sites (1-9), biomass sites (red arrows at mobile sites 1 & 4, stable sites 3 & 6, and control sites 10 & 11), and the location of offshore grab sample transects (A-L).

Nine shell ridge sites were chosen as study locations to examine shell ridge migration and impact to marsh platform soil and vegetation. At each location, stakes were driven into the marsh approximately 5 m landward of each ridge, providing a reference point for tracking shell ridge migration. A standardized protocol of photography was also established for the sites so that images could be directly compared to one another and provide a record of ridge evolution. Photography was completed at each site a total of five times between June 9, 2017 and January 10, 2018.

2.2 Shell Ridge Translation, Area, and Volume Measurements

Measurements of each shell ridge location, height, and translation across the marsh platform were taken four times: July 26, 2017; September 13, 2017; October 11, 2017; and January 10, 2018. However, only five sites were examined on the January visit.

Positional information was obtained with a *Trimble R8* Global Navigation Satellite System (GNSS) with a horizontal and vertical accuracy of $\pm 0.25 \text{ m} + 1 \text{ ppm RMS}$ and $\pm 0.50 \text{ m} + 1 \text{ ppm RMS}$, respectively. The hand held system was used to trace the periphery of each shell ridge multiple times, as well as used to measure the width and height of the ridges.

Early in the study it was recognized that ridges could be differentiated into three groups: isolated ridges, semi-isolated ridges, and non-isolated ridges. Isolated ridges were considered bodies of shell with a clear spatial separation from other shell bodies. Semi-isolated ridges were partially connected to other adjacent ridges, but typically showed a change in width before passing into an adjacent ridge. Non-isolated ridges were recognized as ridges that laterally merged with other ridges making their boundaries challenging to delineate at times. For non-isolated ridges, a boundary was established by moving laterally in both directions along the ridge from the center (stake) and capturing enough body to obtain the general shape of the ridge.

Width and elevation measurements were taken along transects oriented perpendicular to the strike of the shell ridge into the interior marsh. Stakes placed at the beginning of the field effort served as permanent markers at each study site. Measurements were taken once at each ridge during each field visit, except for Ridge 6 which was large and variable in height and three different transects were taken on January 10th.

Length, width, and height data collected for each of the ridges were used to calculate volumes. This was done by determining the cross sectional area of a “slice” of the shell ridge and multiplying that by height and width measurements. These “slices” were separated into rectangles by finding the average of two heights and multiplying it by the length of width that averaged height spanned. The areas of all of the rectangles were summed to give a complete height times width of the whole “slice” and, as most ridge heights were uniform along the length of the ridge, that area of the “slice” was multiplied by the length of the ridge. Only Ridge 6 had varying heights and on 1/10/18 multiple transects were taken to account for this.

In addition, *ArcMap 10.3.1* was used document the shell ridge movement and calculate the changes in ridge area through time. The software was also used to display centroid circles (circle that depicts a body’s center of mass) that could give further insight of the direction and magnitude of shell ridge translation. Wind data was gathered from NOAA (climate.gov) to try to correlate primary wind directions, and thus larger wave activity, with significant ridge movement.

Lastly, Louisiana’s coastline is microtidal, and consequently tidal corrections were not used in any shoreline analysis.

2.3 Shell Analysis

Samples of all shell species present were harvested directly from the crest of each shell ridge and brought back to the laboratory for identification and radiocarbon dating. Twelve shells were chosen for radiocarbon dating to help isolate the source of the shells (e.g. modern or relict shells) and samples for dating were sent to *DirectAMS*. A Gulf Coast reservoir correction of 500 +/- 300 ¹⁴C years BP (Törnqvist, 2015) was not considered to be significant. The focus was to determine whether shells were relatively modern (last 100 years) or ancient and temporally more equivalent to the St. Bernard delta lobe (active ~3.5-1.5 ka).

Additionally, between June 9, 2017 and January 10, 2018, field observations and photographic analysis focused on evaluating the abundance of shell species across each of the sites, as well as the degree of shell fragmentation through time. Specifically, these were determined by direct examination of shell assemblage photographs from each site and estimating the percentage of each shell species and the percentage of shell fragmentation. Observations noted in the field were used to cross check and confirm that entire sites mimicked what was seen in the photographs.

2.4 Grab Samples

Grab samples were taken offshore of Little Bayou Pierre to determine if the shallow nearshore seafloor contained shells and was contributing to the volume of the onshore shell ridges. Grab samples were taken using a *Wildco Petite Ponar*, with a 2.4 liter volume and a 6 x 6 in sample area. Upon measuring the instrument, it was estimated that its sample collection extracted from the top 10 cm of substrate. The grabs from this Ponar were taken along twelve 0.5 km-long transects perpendicular to the shell ridges and the shoreline, with five grab samples taken along each transect, with 100 m separation. Locations were logged using a *Garmin*

GPSmap 60 Cx. Each grab sample was brought back to the laboratory to determine sediment characteristics and the percentage of shell content.

2.5 Marsh Biomass Analysis

Two independent assessments of marsh health relative to the presence or absence of shell ridges was conducted at each of three different types of shell ridge conditions: a) marsh platform with no shell ridges, b) marsh platform with stable ridges, and c) marsh platform with mobile ridges. Ridges were determined to be a mobile ridge if movement into interior marsh was more than 5 m during the ~2.5 month time frame of 7/26/17 to 10/11/17 and stable if translation was less than 5 m.

At each of these three types of locations, four 1 m x 1 m plots were set up along a transect with increasing distance into the interior marsh to obtain above- and belowground biomass. The first plot was set right at the shoreline, the second was set 5 m inland, the third was set 10 m inland and the fourth was set 35 m inland.

Above- and belowground biomass analysis followed a combination of methods and strategies presented by Gallagher (1974), Schubauer and Hopkinson (1984), and Darby (2006). For aboveground biomass, a 0.25 m x 0.25 m section of the plot was used to harvest stems of marsh vegetation. Vegetation was cut at the sediment interface, placed into bags, and brought back to the laboratory where live (various shades of green) and dead (yellow, tan, or brown), vegetation was separated, heated at 60°C for ~12 hours to drive off water content, then weighed.

Similarly, belowground biomass was determined by taking 50-cm long x 7.5-cm diameter push cores in the remaining part of the plot. In the laboratory, the marsh soil and biomass inside the core was separated with a 1 mm sieve so that only root and rhizome material remained. Root

and rhizome material was then separated into live (white and turgid) and dead components (dark brown or gray and flaccid), each of these were then dried ~12 hours at 60°C and then weighed.

2.6 Aerial and Satellite Imagery for Geomorphic History

Aerial and satellite imagery from 1965-2015 was also used to gain an understanding of the geomorphic history of Little Bayou Pierre. Imagery from 2015, specifically, was also used to analyze a section of Biloxi Marsh with the purpose of measuring shorelines with and without shell ridges. This was done in order to evaluate what percentage of shoreline in the Biloxi Marsh might be affected by shell ridge presence. Images were collected from Edgar Tobin Aerial Surveys and *Google Earth*.

CHAPTER 3. RESULTS

3.1 Shell Ridge Translation, Area, and Volume Measurements

The magnitude of shell ridge translation across the marsh platforms varied between the sites (Table 1, in appendix; Fig. 8). Ridges 2, 3, 4, and 9 were only measured on 7/26/17, 9/13/17, and 10/11/17, whereas Ridges 1, 5, 6, 7, 8 were measured on 7/26/17, 9/13/17, 10/11/17, and 1/10/18. It should be noted that Ridge 2 consisted of two very small ridges, which are at times referred to as 2a (located northeast) and 2b (located southwest). The magnitude of lateral translation could be documented for 2a and 2b, however, elevation transects were only acquired for 2a, so volume measurements referring to 2 is the volumetric quantification of 2a. Area measurements were able to be made for 2a and 2b using ArcMap.

Figure 8 shows the magnitude of all the ridge movements, which ranged from -0.55 m (Ridge 3) to 37.94 m (Ridge 8). Ridge 3 was the only site to show a negative movement. This does not necessarily mean a translation closer to the shore, but most likely is the result of different water heights changing the delineation of the shoreline at a very stable ridge. In addition, Ridge 8 showed more significant movement (40.76 m) on 10/11/17, however, it is believed from field observations and photography that some amount of data points were erroneously dropped from the dataset and that these data points would have shown a less significant amount of movement. Therefore, it can be most safely concluded that 37.94 m was the highest movement seen amongst all shell ridges.

All ridges were compared from the time period of 7/26/17 to 10/11/17 to determine which ridges were stable and which were mobile. Table 1 (in appendix) shows the results. Ridges 2a, 2b, 3, 6, 7, and 9 were considered stable (Fig. 9), whereas Ridges 1, 4, 5, and 8,

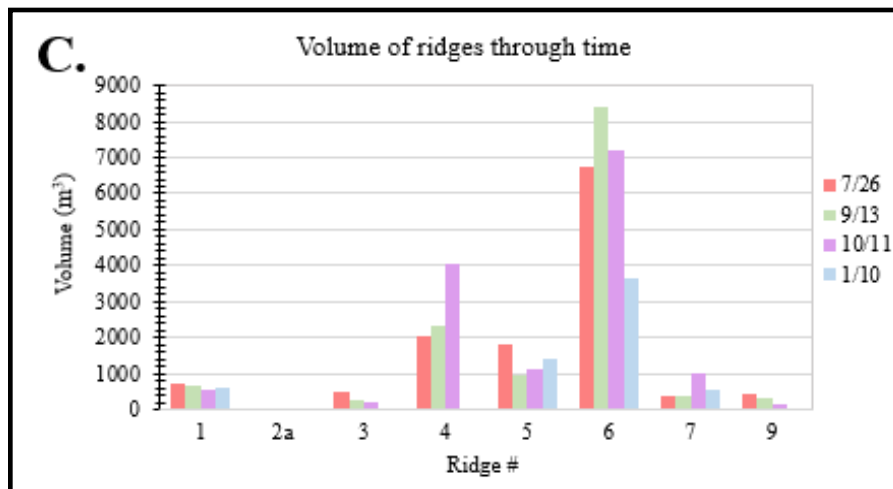
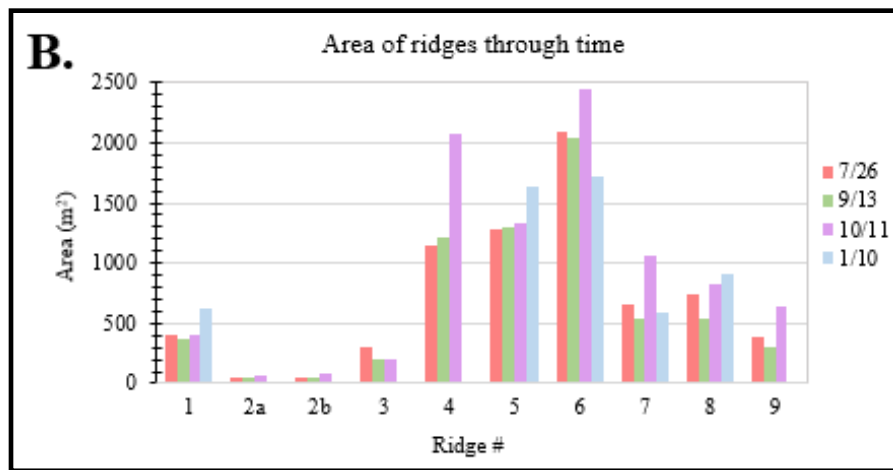
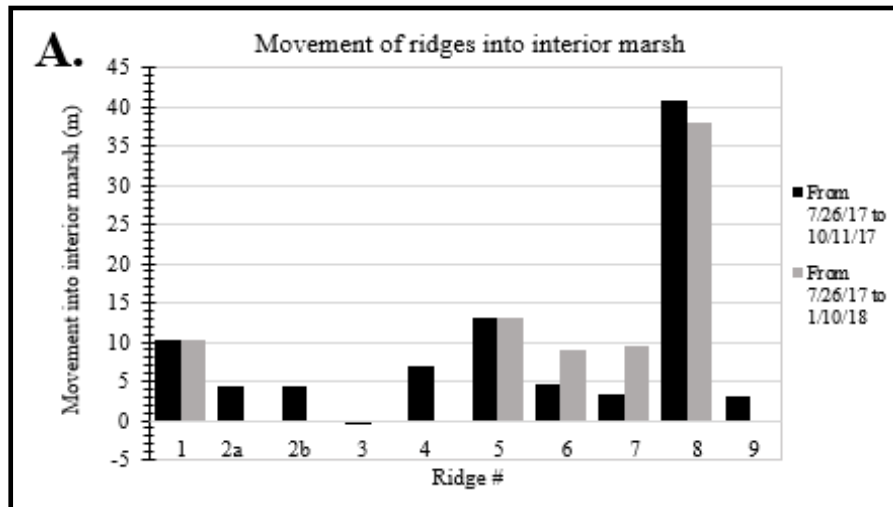


Figure 8: (A) Plot showing the magnitude of translation of ridges into the interior marsh platform during two different time periods. All of the ridges were measured from 7/26/17 to 10/11/17, however, ridges 1, 5, 6, 7, and 8 were also measured between 7/26/17 and 1/10/18. (B & C) Plots showing the total area of ridges and volume of ridges through time, respectively. Volume measurements for 2b and 8 could not be obtained due to transects not being taken at those sites.

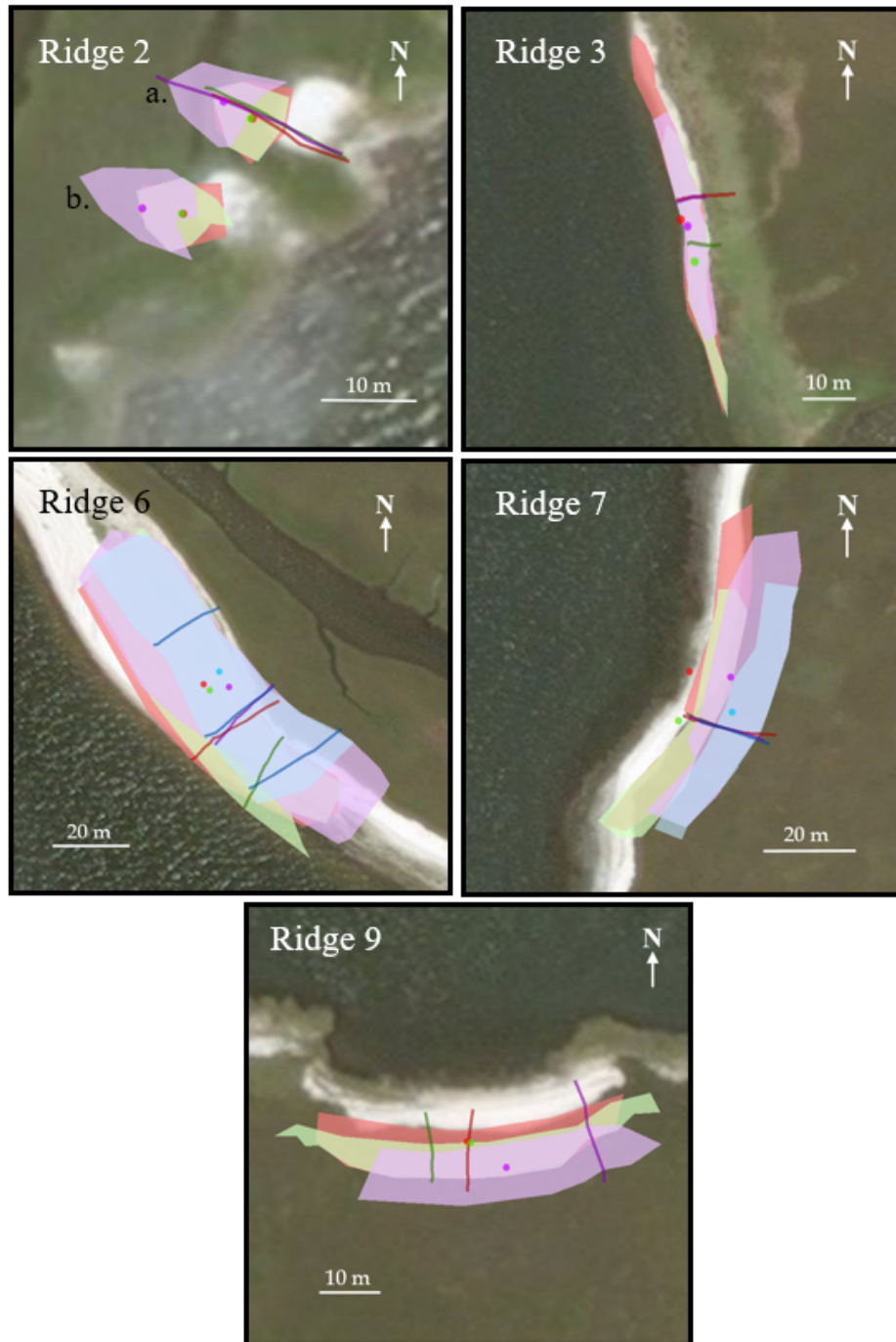


Figure 9: Maps of six different stable shell ridges (2a, 2b, 3, 6, 7, and 9), where the polygons of various colors represent shapes and locations of these shell ridges through time. 7/26/17 (Red), 9/13/17 (Green), 10/11/17 (Purple), and 1/10/18 (Blue). Ridges were considered stable if translation of the shell ridge into the interior marsh from 7/26/17 to 10/11/17 was less than 5 m.

Lines of various colors represent the temporally corresponding elevation transects taken across the shell ridges during successive field visits and the colored circles represent temporally corresponding centroid circles of each of the polygons formulated using *ArcMap 10.3.1* (imagery from *DigitalGlobe*, 7/7/2016).

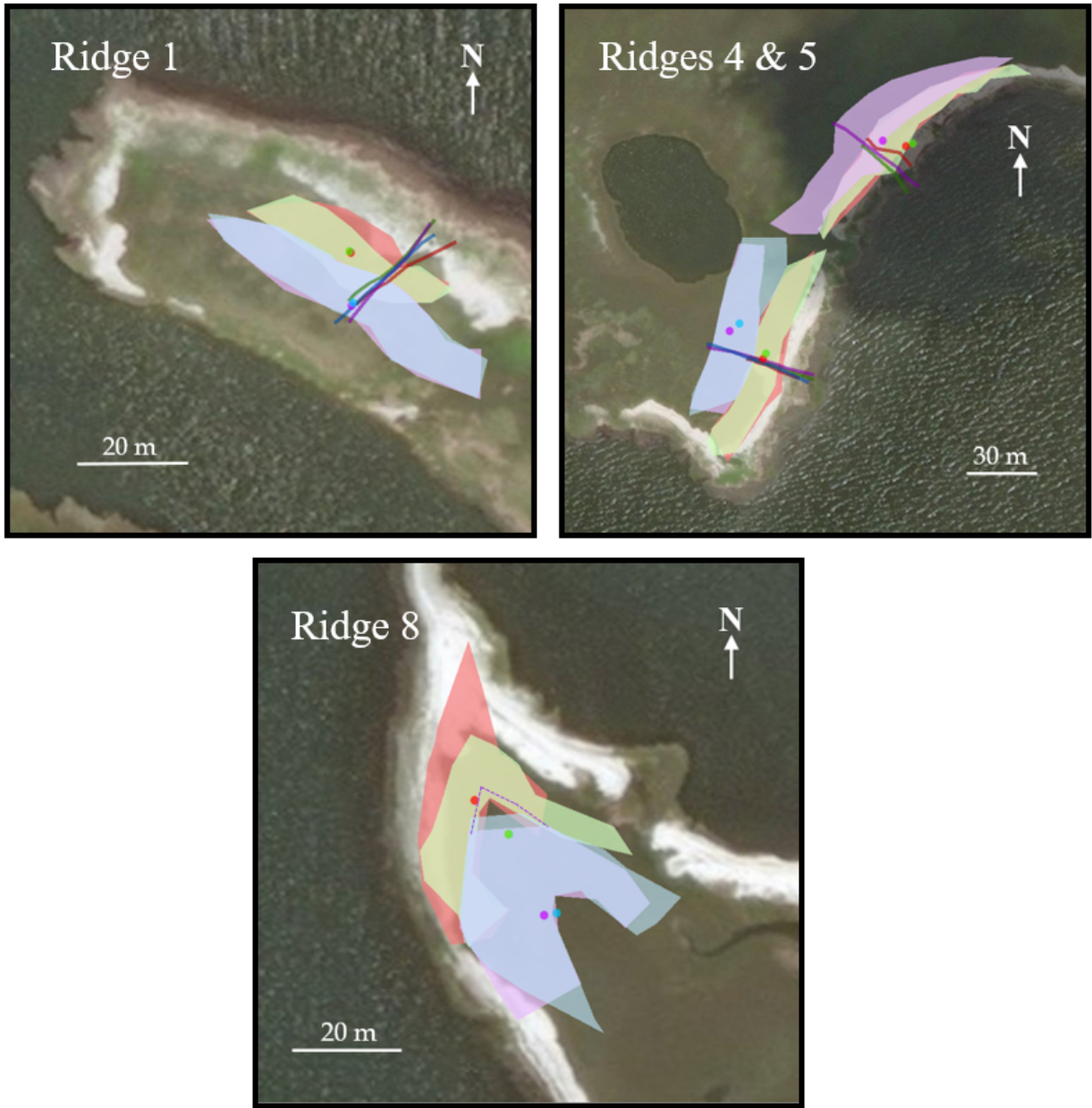


Figure 10: Maps of four different mobile shell ridges (1, 4, 5, and 8), where the polygons of various colors represent shapes and locations of these shell ridges through time. 7/26/17 (Red), 9/13/17 (Green), 10/11/17 (Purple), and 1/10/18 (Blue). Ridges were considered mobile if translation of the shell ridge into the interior marsh from 7/26/17 to 10/11/17 was more than 5 m. Note that Ridge 8 on 10/11/17 has a dotted line where the shell ridge is believed to have extended. Field observations and photography cause the belief that some data points are missing in the data set.

Lines of various colors represent the temporally corresponding elevation transects taken across the shell ridges during successive field visits and the colored circles represent temporally corresponding centroid circles of each of the polygons formulated using *ArcMap 10.3.1* (imagery from *DigitalGlobe*, 7/7/2016).

were considered mobile (Fig. 10).

The area of shell ridges ranged from 48 m² to 2,439 m² (Table 3, in appendix; Fig. 8). From 7/26/17 to 9/13/17, most ridges lost area, whereas from 9/13/17 to 10/11/17 and from 10/11/17 to 1/10/18 most ridges gained area. The volume of shell ridges had an even larger range of 42 m³ to 8419 m³ (Table 3, in appendix; Fig. 8). Half of the ridges gained volume and half lost volume from 7/26/17 to 9/13/17, whereas between 9/13/17 and 10/11/17, five of eight ridges lost volume. From 10/11/17 to 1/10/18, half of the four ridges measured lost volume and half gained volume.

In addition, centroid circles clustered together without much separation where ridges were stable and showed more separation where ridges were mobile. The largest offset of centroids was during the period 9/13/17 to 10/11/18.

Wind data showed that the primary wind directions were N-NNE from 7/26/17 to 9/13/17, NE-ENE and S-SSE from 9/13/17 to 10/11/17, and N from 10/11/17 to 1/10/18 (Figs. 11, 12, and 13).

3.2 Shell Analysis

The shells harvested from ridge crests were identified as *Anadara brasiliiana*, *Anadara transversa*, *Busycon pulleyi*, *Dinocardium robustum*, *Crassostrea virginica*, *Cyrtopleura costata*, *Geukensia granosissima*, *Littorina irrorata*, *Neverita duplicata*, *Rangia cuneata*, and *Tagelus plebeius*. The habitats of these shells consist of a wide range of environments including: marshes, bays and bay margins, estuaries, and offshore regions extending from the shoreline to 75 m deep (Tunnell et al., 2010).

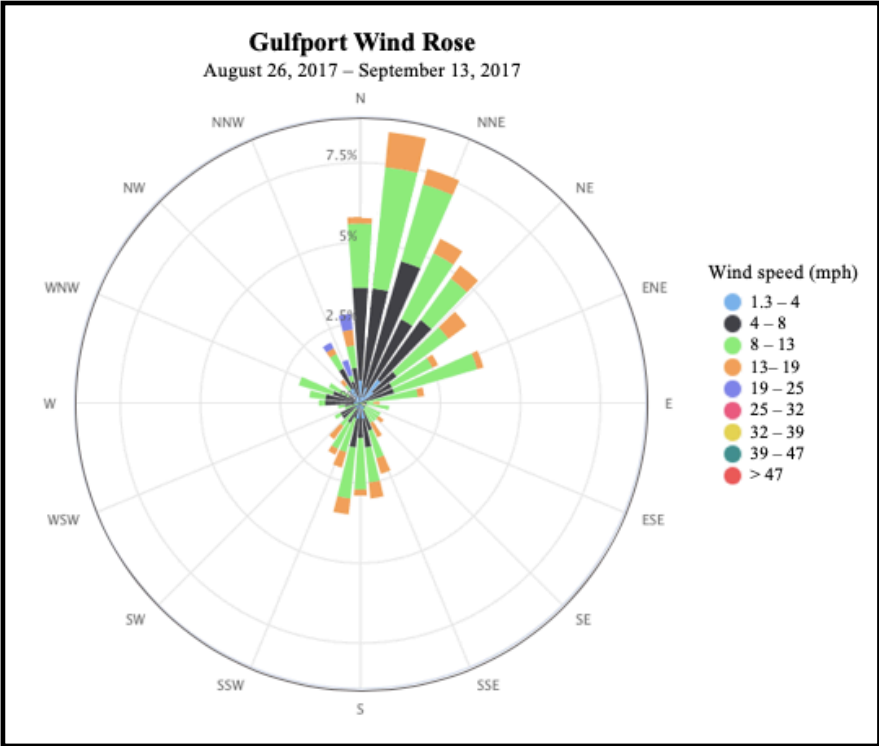


Figure 11: Wind rose diagram showing dominant wind speeds from Gulfport, Mississippi for the time period between August 26, 2017 and September 13, 2017.

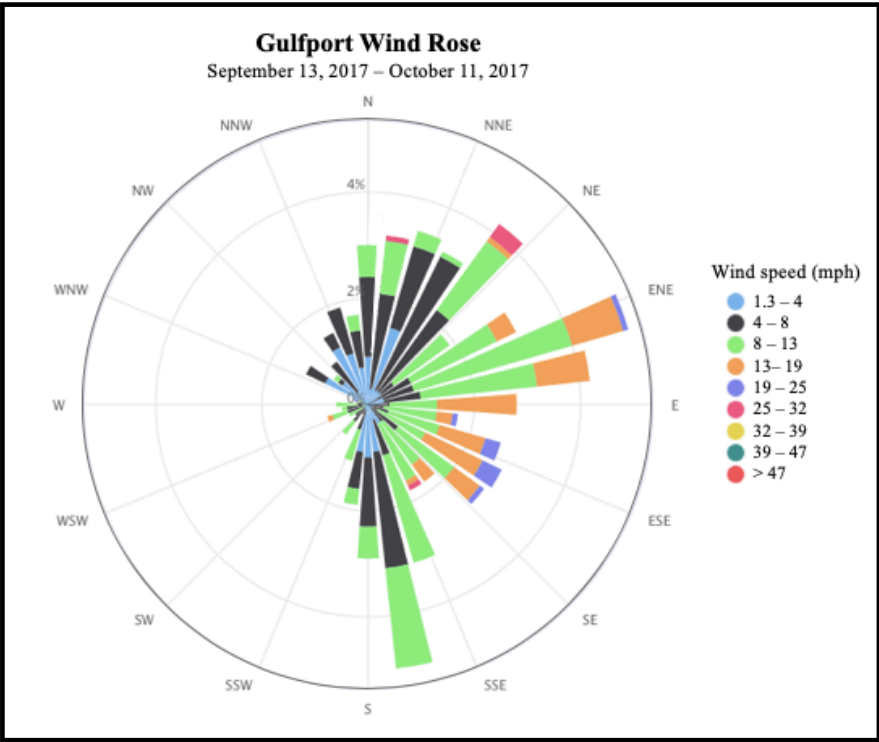


Figure 12: Wind rose diagram showing dominant wind speeds from Gulfport, Mississippi for the time period between September 13, 2017 and October 11, 2017.

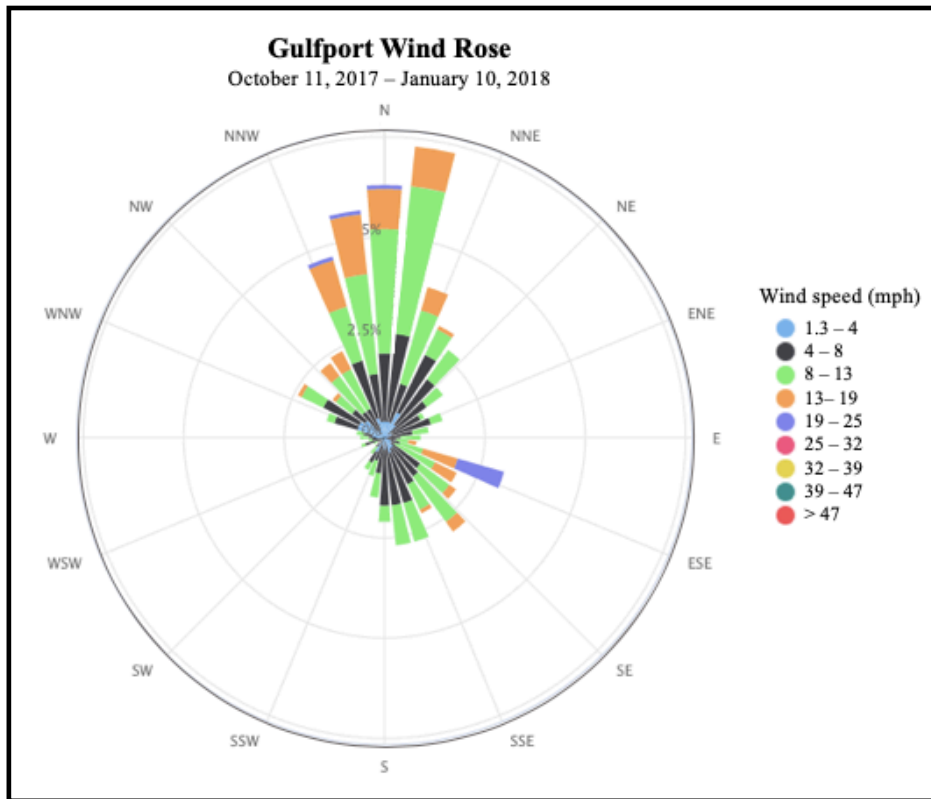


Figure 13: Wind rose diagram showing dominant wind speeds from Gulfport, Mississippi for the time period between October 11, 2017 and January 10, 2018.

Direct observations of shell ridges showed that Ridges 1-5 and Ridge 8-9 were overwhelmingly dominated by *Crassostrea virginica* shells (85-95%). However, Ridges 6 and 7 consisted of ~50% *Crassostrea virginica* and ~50% *Rangia cuneata*. In addition, from June 9th to January 10th, the shells in Ridges 1, 2, 4, 5, and 9 showed more fragmentation through time than shells from Ridge 7. Shells from Ridges 3 and 8 remained fragmented, and shells from Ridge 6 remained whole.

Interestingly, radiocarbon dates for *Crassostrea virginica* from Ridges 2, 3, 5, 6, 7, 8, and 9 ranged from 832 +/- 22 years BP to modern (modern refers to 1950 A.D.) and *Rangia cuneata* from Ridges 6, 7, and 9 were dated to 2125 +/- 28 years BP, 2138 +/- 23 years BP, and 2092 +/-

22 years BP respectively. Furthermore, a *Dinocardium robustum* shell from Ridge 2 was dated to modern; an *Anadara brasiliana* shell from Ridge 4 was dated to 597 +/- 25 years BP (Table 4).

Site	Species	Age (yr BP)
2	<i>Crassostrea virginica</i>	Modern
2	<i>Dinocardium robustum</i>	Modern
3	<i>Crassostrea virginica</i>	832 +/- 22
4	<i>Anadara brasiliana</i>	597 +/- 25
5	<i>Crassostrea virginica</i>	Modern
6	<i>Crassostrea virginica</i>	269 +/- 26
6	<i>Rangia cuneata</i>	2125 +/- 28*
7	<i>Crassostrea virginica</i>	454 +/- 21
7	<i>Rangia cuneata</i>	2138 +/- 23*
8	<i>Crassostrea virginica</i>	827 +/- 20
9	<i>Crassostrea virginica</i>	Modern
9	<i>Rangia cuneata</i>	2092 +/- 22*

Table 4: Uncalibrated radiocarbon dates of shells at several of the shell ridge study sites, presented in years “before present” (BP). Modern refers to the date of 1950 A.D., indicating that the dated material was approximately equal to or less than 68 years old. Asteriks (*) denote shells with ages corresponding to the age of the St. Bernard delta lobe.

3.3 Grab Samples

A surprising find of the offshore grab sampling effort was that 73% of the samples had low percentages of shell content with 44 out of 60 samples containing only 0-20% shell content. (Fig. 14). Only 9 samples had shell percentages of 81-100% and these samples were randomly distributed offshore, as were the remaining 7 samples that ranged between 21-80% shell content.

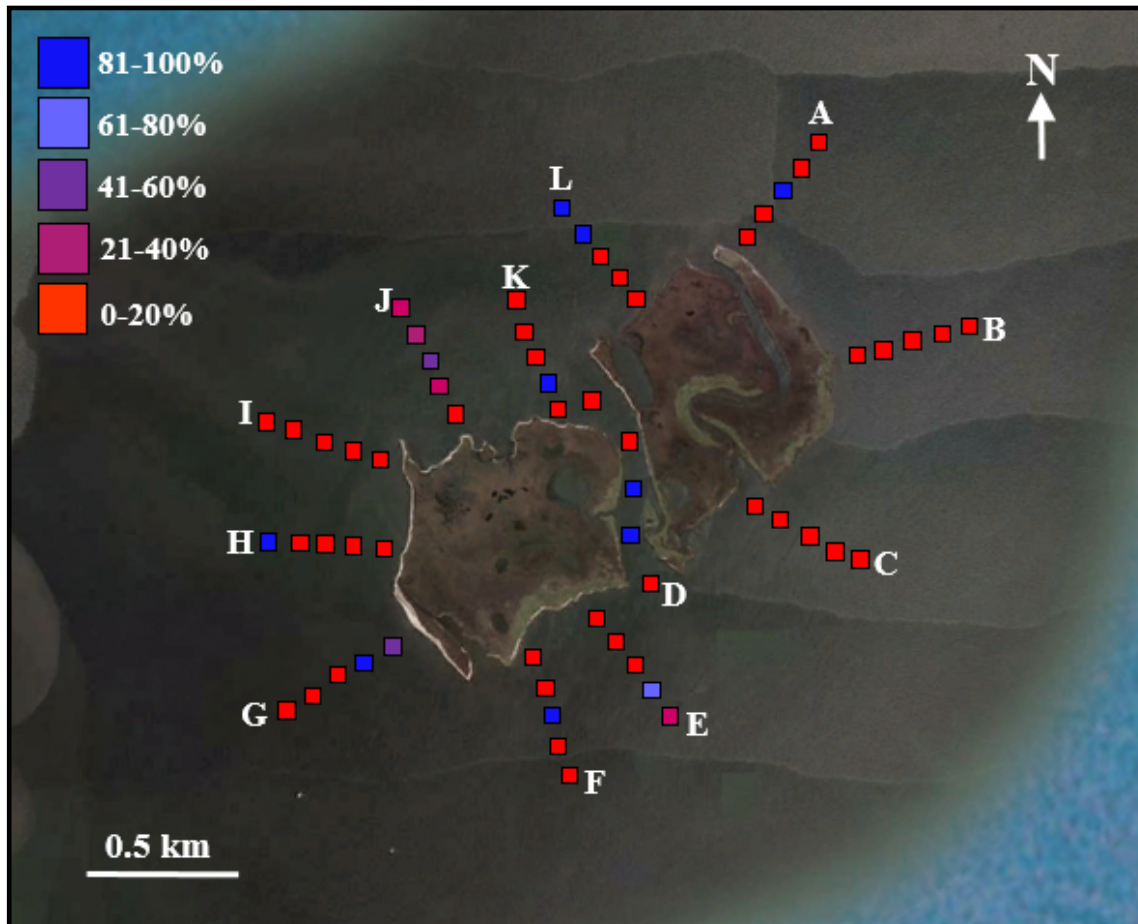


Figure 14: Base map of grab sample transects and each of the grab sample locations. Locations indicated with a red box represents a low percentage of shell content (0-20%) in the grab sample, whereas blue represents a high percentage of shell content (81-100%). Note the relative lack of shells captured within each of the grab samples.

3.4 Marsh Analysis

3.4.1 Aboveground biomass

3.4.1.1 Sites without a ridge

Aboveground biomass results (Fig. 15) showed that sites without a ridge (10 & 11) had the highest combined average total (alive and dead) biomass (33.73 +/- 25.65 g) compared to mobile (29.38 +/- 42.62 g) and stable ridge (8.40 +/- 11.49 g) sites, with every sample plot along each transect at these sites yielding some biomass (ranging from 5.62 g to 71.44 g). Site 10 primarily consisted of dead biomass. Site 10 biomass sample plots along the shoreline, at 10 m,

and 35 m inland had significantly less dead biomass than at 5 m inland, with plots at 10 m and 35 m placed where interior ponding was present. Both alive and dead biomass at Site 11 increased with distance into the interior marsh.

3.4.1.2 Sites with a stable ridge

Sites with a stable ridge (3 & 6) showed the highest masses of alive and dead vegetation at any site, both of these peaks located immediately behind the width of their respective ridges (at 5 m for Site 3, at 35 m for Site 6). At both shoreline plots for Sites 3 & 6, no data was able to be collected because of the ridge thickness that rendered the shell mass unmovable with available tools. This also made it impossible to conduct belowground biomass analysis at this site. It is important to note that at Site 3, there was interior ponding recorded at 35 m inland and at Site 6, there was no aboveground biomass present 5 m or 10 m along the transect. The width of the ridge at Site 6 extended to the area between 10 m and 35 m, so that plots at 5 m and 10 m were placed inside the width of the shell ridge, however, the shell material blanketing the surface at these plots was short enough to dig and obtain data.

3.4.1.3 Sites with a mobile ridge

Sites with a mobile ridge (1 & 4) had extremely low amounts of both alive and dead aboveground biomass at the majority of plots with an average total biomass of 8.40 +/- 11.49 g. At Site 1, the shoreline plot was placed over marsh that did not have shells present even at the beginning of the study, so it is assumed that shells were once present there, but had already moved inland by the start of the study. No aboveground biomass was present at the shoreline. At 5 m and 10 m inland at Site 1, the shell ridge was no longer present (shell ridge was present over 5 m on 7/26/17 and over 10 m on 9/13/17). It was not noted in the field, but it is assumed that the ridge was entirely present between 10 m and 35 m by the time the biomass data was being collected based on the fact that the shell ridge was present between 10 m and 35 m at the last

recorded movement (1/10/17). No aboveground biomass was present at 5 m and the total biomass at 10 m yielded 15.88 g. At 35 m inland, behind the mobile shell ridge, the total biomass increased to 30.65 g. At Site 4, biomass was not present at shoreline, and extremely low at 5 m and 10 m, all of which were before the main bulk of the shell ridge, and at 35 m, past the main bulk of shell ridge, there was a significant increase in alive biomass to 16.99 g. Interestingly, this plot (35 m) was located between more heavily vegetated marsh to either side.

3.4.2 Belowground biomass

3.4.2.1 Sites without a ridge

Belowground biomass was relatively consistent for sites without ridges (10 & 11), averaging 45.80 +/- 23.62 g. (Fig. 15). These sites showed no consistent increase or decrease along transects for alive or dead belowground biomass.

3.4.2.2 Sites with a stable ridge

Sites with stable ridges (3 & 6) also showed consistent belowground alive and dead biomass numbers. These sites had a combined average of 32.78 +/- 7.40 g of total biomass, the lowest at 23.14 g and the highest at 40.71 g. At stable site 3, dead belowground biomass decreased with distance into the marsh from the marsh edge, whereas for site 6, alive biomass increased and dead biomass decreased as plots increased distance into the marsh.

3.4.2.3 Sites with a mobile ridge

For sites with mobile ridges (1 & 4), total biomass was fairly consistent, except one large peak of 60.41 g at the shoreline of Site 1. The combined average of total biomass at sites 1 and 4 was 28.80 +/- 14.32 g, lower than both sites without a ridge (45.80 +/- 23.62 g) and sites with a stable ridge (32.78 +/- 7.40 g). Alive biomass averaged 6.09 +/- 3.41 g, lower than sites without ridges, 14.52 +/- 5.51g, and sites with stable ridges, 14.70 +/- 5.72 g. Dead biomass averaged

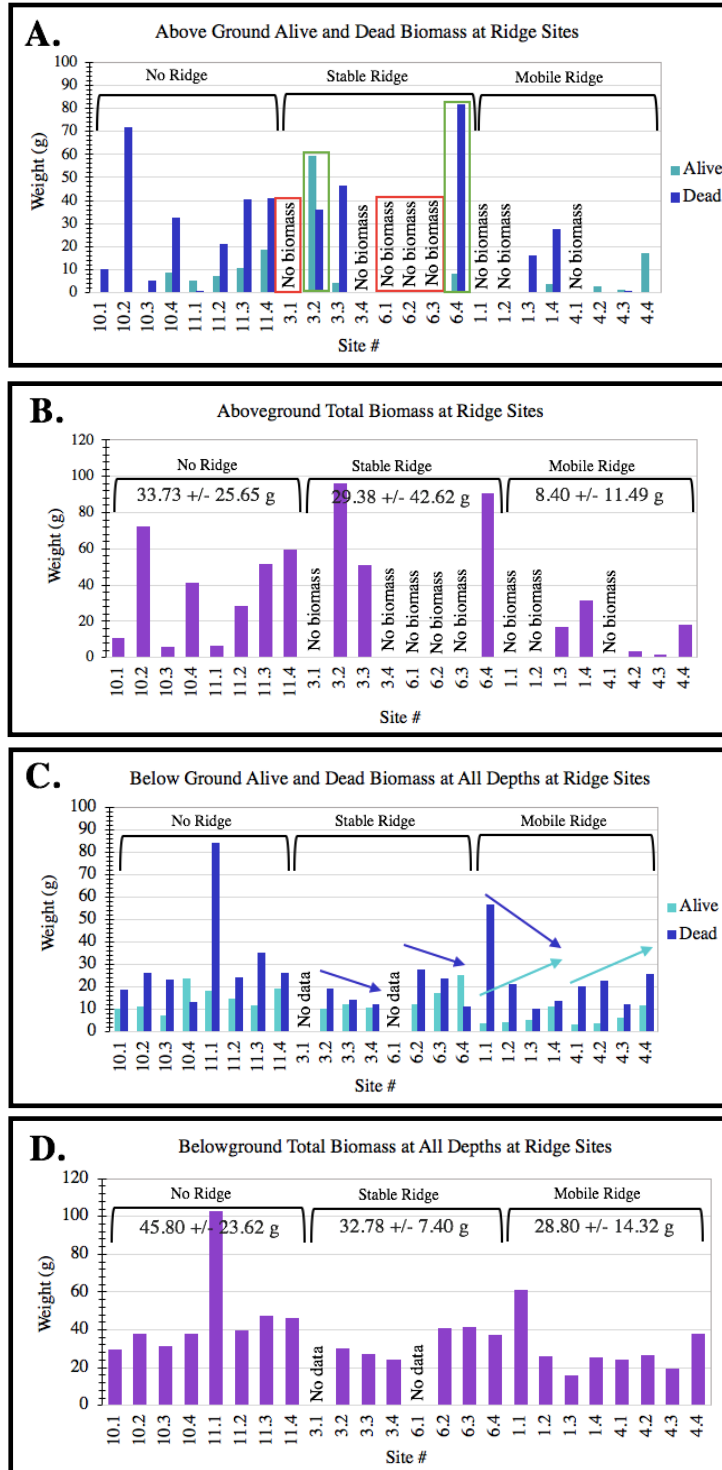


Figure 15: Biomass data for each of the sampled locations. Transects are represented by decimals (e.g. 10.1 = shoreline, 10.2 = 5 m inboard, 10.3 = 10 m inboard, 10.4 = 35 m inboard). (A) Aboveground biomass separated into alive (teal) and dead (indigo) fractions. Red boxes identify plots with shell ridge presence above it and green boxes surround the high peaks of alive and dead biomass behind stable shell ridges. (B) Total (alive and dead) aboveground biomass weights. (C) Belowground biomass, separated into alive (teal) and dead (indigo) weights. Arrows represent increasing or decreasing amounts of alive (teal) or dead (indigo) biomass as distance into the marsh increases. (D) Total (alive and dead) belowground biomass weights.

22.70 +/- 14.74 g, more similar to other two types of sites, 31.28 +/- 22.30 g for sites without ridges and 18.09 +/- 6.64 g for sites with stable ridges. For Site 1, alive biomass increases with increasing distance into the interior marsh and dead biomass decreases along the first three plots. For Site 4, alive biomass also increases with increasing distance into the interior marsh.

3.4.3 Data analysis

Hypothesis testing was conducted for all sites to evaluate if the results are statistically significant. Statistical analysis among sites using t-tests show that aboveground biomass yield p-values of 0.81 (site without a ridge and site with a stable ridge), 0.22 (site with a stable ridge and site with a mobile ridge), and 0.03 (site without a ridge and site with a mobile ridge). For belowground biomass, the p-values ranges from 0.18 (site without a ridge and site with a stable ridge), 0.51 (site with a stable ridge and site with a mobile ridge), and 0.11 (site without a ridge and site with a mobile ridge) respectively.

3.5 Aerial and Satellite Imagery

Aerial and satellite imagery of Little Bayou Pierre revealed a consistent reduction in land area from 1965 to present, as well as a correlation between presence or absence of shell and marsh edge stability or erosion (Fig. 16). The 1965 image shows the largest island footprint of all available imagery (~2.01 km²) with most shell ridges concentrated along the north side of the island and parts of the interior channel between the two islands. By 1989, the shell ridges had become more extensive, accumulating along the west edge as well. Widths of shell ridges are presented in Table 5. By 2004, the shell ridges had accumulated along the entire west edge, continued to accumulate along the interior channel, and began to accumulate along the south edge. An image from October 2005 after Category 3 Hurricane Katrina of August 2005 shows significant erosion of the island, particularly along its north and east sides and the shell ridges on the west side overwashed ~44 m inland. In 2009, the shell ridges again coalesced along the shore

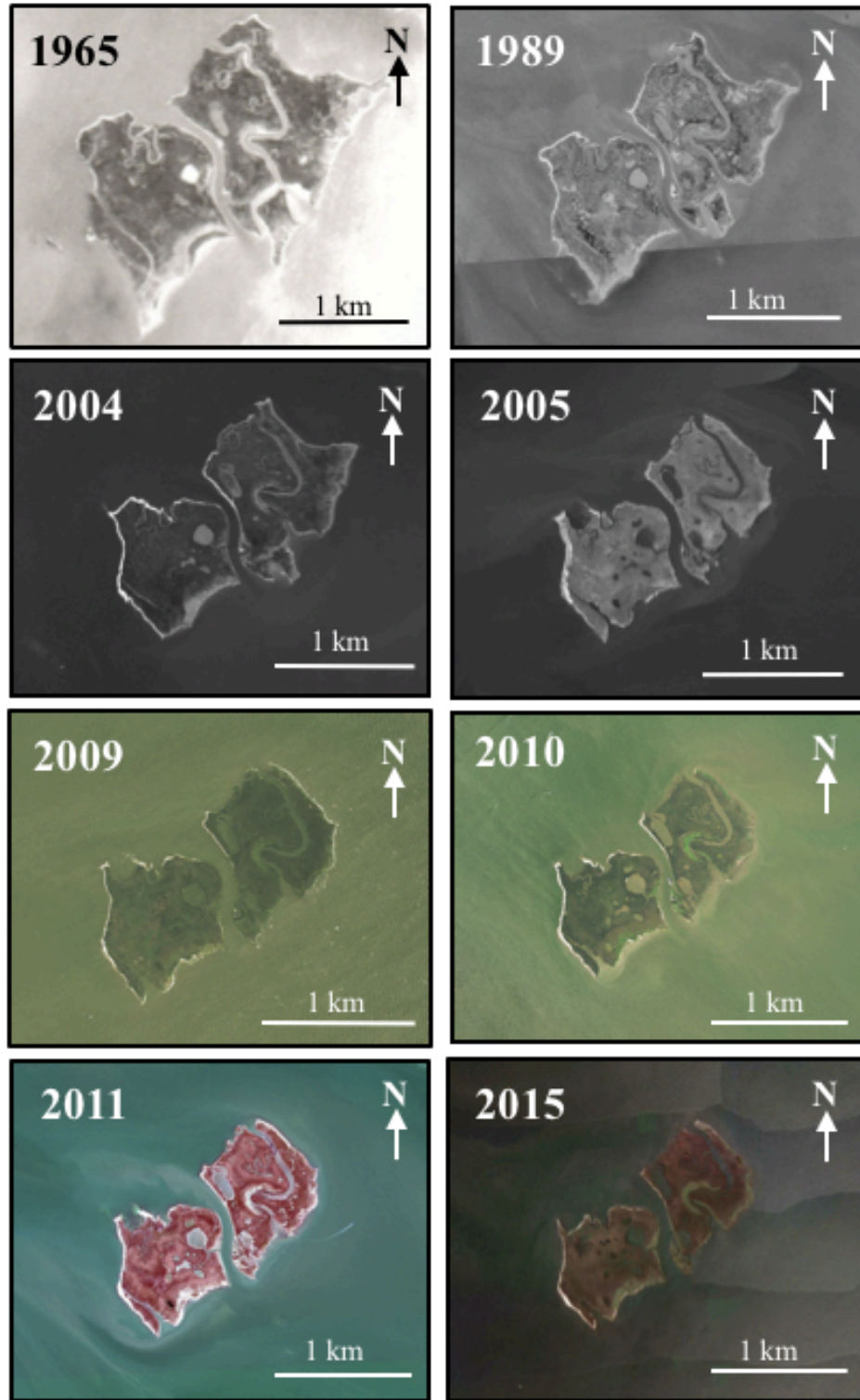


Figure 16: Aerial and satellite imagery showing the morphologic change of Little Bayou Pierre: 1965 (Tobin Aerial Surveys), 1989, 2004, 2005, 2009, 2010, 2011, 2015 (from *Google Earth*). Note the consistent reduction in the island footprint and the stability of the western side of Little Bayou Pierre, where shell ridges are extensive, compared to the eastern side where they are absent.

Year	Shell Ridge Width from Satellite Imagery (m)		
	West	Interior	East
1989	14.87	8.94	3.91*
2004	34.89	6.52	0
2005	21.99	4.04	0
2009	14.79	5.38	3.89
2010	24.49	10.74	0
2011	32.99	13.73	4.28*
2015	2.73	3.73	0

Table 5: Shell ridge widths from 1989 to 2015 as measured from satellite imagery (*Google Earth*). These widths were taken along the western side, the interior channel, and the eastern side of Little Bayou Pierre. Stars (*) note where imagery up close was hazy and hard to distinguish, providing doubt about the presence of shell ridges at that time.

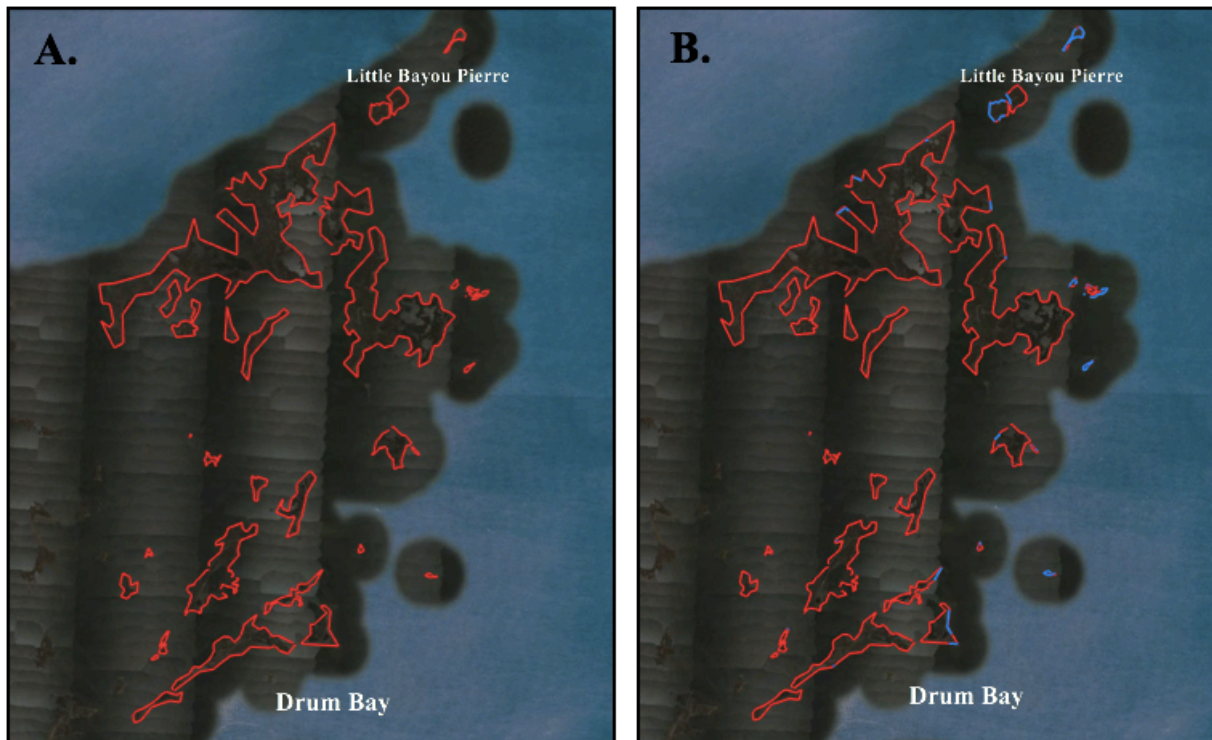


Figure 17: Satellite imagery (*Google Earth*, 2015) indicating measured shorelines in the northeast Biloxi Marsh. (A) Red lines represent total measured shoreline. (B) Blue lines represent the portion of total shoreline with shell ridges present in 2015.

and appear to extend down the eastern side as well as the western side. By 2010, the shell ridges became wider along the west edge and interior channel and have eroded away on the east side or possibly submerged and capped with mud. Lastly, in the images from 2011 to 2015, a decrease

in size and extent of shell ridges is evident and the smallest island footprint of all the imaged years is seen in 2015 (~0.96 km²). The change in island area from 1965 to 2015 yielded 0.73 km² of total land loss and a rate of 0.02 km² per year. Shoreline retreat from 1989 to 2015 was compared for the west edge, which retreated 119 m, and the east edge, which retreated 433 m.

Lastly, the percent of Biloxi Marsh shoreline that is fringed by shell ridges was able to be estimated. Shoreline measured from Drum Bay to the most northeastern tip of the Biloxi Marsh, near Little Bayou Pierre (Fig. 17), indicated that out of 200.39 km of shoreline, 14.35 km of shoreline was fringed with shell material (7.16%).

CHAPTER 4. DISCUSSION

4.1 Shell species, origin, and marsh-edge accumulation

Most of the shell ridges examined in this study consisted of predominantly *Crassostrea virginica*, which were relatively young in age, less than 1.0 ky. *Crassostrea virginica* is an estuarine species that has a wide salinity tolerance, but favors environments of 10-28 ppt (Shumway, 1996). Three out of seven radiocarbon-dated shells yielded modern ages of less than approximately 70 years, which points to nearby local man-made oyster fisheries or natural oyster reefs as probable sources. The absence of shell material in offshore grab samples 0.5 km seaward of the marsh edge, suggests that shells are sourced from local sedimentary horizons deeper than the sampling capability of the grab sampler (>10 cm) and possibly placed onshore in periodic episodes depending on availability of shell material offshore. The second most common species was *Rangia cuneata* shells. In agreement with Ellison's (2011) models, these shells are likely being excavated from the subsurface from St. Bernard delta deposits, as their ages range from 2092 +/- 22 years BP to 2138 +/- 23 years BP, which fit the timeframe of the St. Bernard delta complex development (Törnqvist, 1996). Additional evidence is provided by a U.S. Army Corps of Engineers map (Dunbar et al., 1994), which suggests that the west side of Little Bayou Pierre overlies a paleochannel (Fig. 18), spatially coincident with the terminus of a channel of the St. Bernard delta complex (Rodgers et al., 2009). *Rangia cuneata* species favor very low-salinity, 0-15 ppt river-influenced bay and marsh environments (Tunnell et al, 2010), and have been found in distributary-mouth-bar facies of Lower Grand River, Bayou Lafourche, Louisiana (Frazier, 1967) and Lake Pontchartrain estuary (Poirrier et al., 2008). *Rangia* shells are one of the dominant species of the west ridges found at the Little Bayou Pierre study site and the ravinement of the subsurface channel stratigraphy provides a likely source for the *Rangia* shells.

The results of this provide the following statements to be drawn regarding the transport of shells to the marsh edge:

- (1) **Proximity to source:** shells are originating from locations close enough to the marsh platform that shell excavation and placement onshore by wave energy is feasible,
- (2) **Retreat of marsh shoreline:** shells may be liberated from the sedimentary units underlying marsh (e.g. a relict distributary channel) and become available for onshore transport,
- (3) **Swell energy:** the marsh platform needs to be surrounded by large fetch areas that allow enough swell energy for placement of shell material onshore.

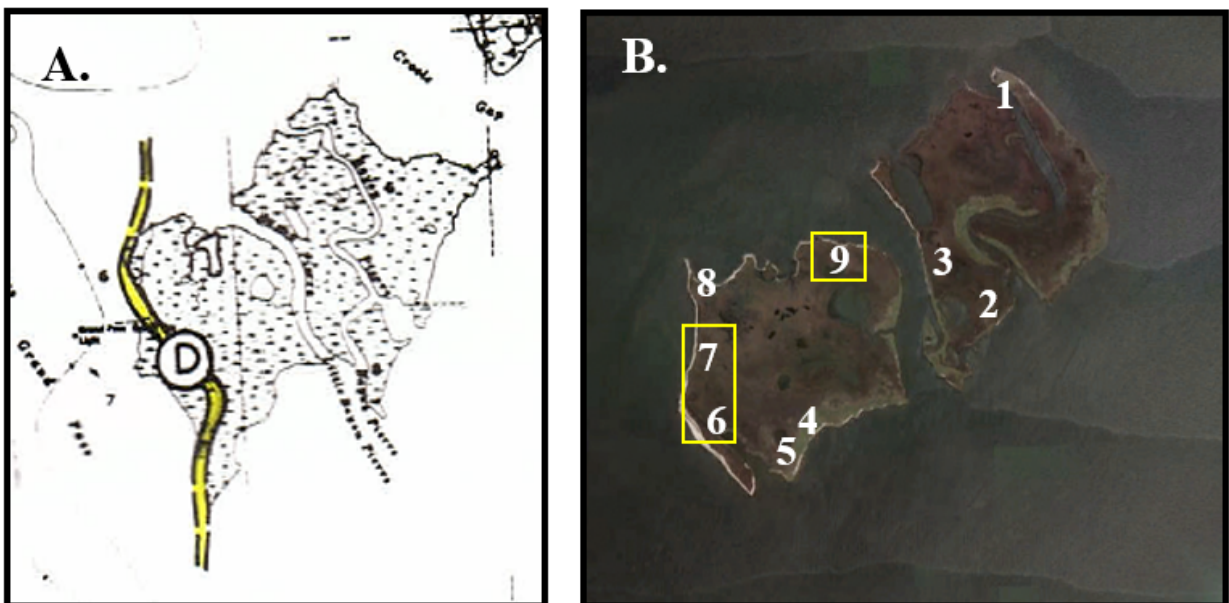


Figure 18: (A) Map illustrating that Little Bayou Pierre overlies a relict distributary channel on its western edge (yellow channel; from Dunbar et al. 1994). (B) Image of Little Bayou Pierre with sites that yielded *Rangia cuneata* shells (ages ranged between 2092 +/- 22 years B.P. and 2138 +/- 23 B.P.) indicated with yellow boxes (2015 imagery from *Google Earth*).

The distributary channel mapped at Little Bayou Pierre by Dunbar et al. (1994) coincides with a St. Bernard distributary channel location mapped by Rogers et al. (2009). The abundance of *Rangia cuneata* shells (approximately half of all the shells) along the western edge of Little Bayou Pierre and dates that correspond to the approximate age of the St. Bernard delta lobe suggests that the distributary channel is a probable source for the *Rangia* shells.

The model Ellison (2011) provided for marsh edge shell accumulations (Fig. 4) was partially adapted from work by Wilson and Allison (2008) on marsh edge erosion and scarp development. In terms of shell accumulation on the marsh edge, this study found disagreement with the Ellison (2011) model describing the stages of formation, suggesting that a modification of the Ellison (2011) model is warranted, particularly Stages B and C. A modified summary of this model (Fig. 19) is provided below:

Stage A: Slowly subsiding marsh.

Stage B: Erosional scarp formed on marsh edge. Liberated sediment becomes suspended and transported onto the marsh surface during elevated water levels through strong wave action and possibly tidal currents.

Stage C: Eventually, large disarticulated and fragmented shell pieces are also transported onshore during stronger energy events (e.g. tropical cyclones) from either the modern seafloor or eroded subsurface.

Stage D1: Stable shell ridge is larger in size, fetch-protected, and/or has more stable subsurface strata, and it locally protects the marsh platform.

Stage D2a: Mobile shell ridge is not overlying stable subsurface strata and/or is in an area with larger fetch.

Stage D2b: Mobile shell ridge washes over the marsh platform, spreading shells and smothering marsh vegetation, resulting in a marsh platform with no vegetative cover and a higher susceptibility to marsh erosion.

Stage D2c: Wave action that is not dampened by aboveground marsh vegetation causes the shells to reaccumulate and erosion causes the shoreline to translate landward.

The first change to the Ellison (2011) model is in a more clearly differentiated set of stages. During Stage B, smaller material is deposited onshore following marsh edge erosion and wave action, whereas during Stage C, larger shell material is deposited onshore following storm events. Previously, Ellison (2011) had combined these two different stages of onshore deposition in Stage B and had included Stage C processes with Stage D, which had described when the shells both protect the marsh and inhibit vegetation growth.

The second change occurs with the separation of Stage D into D1, D2a, D2b, and D2c.

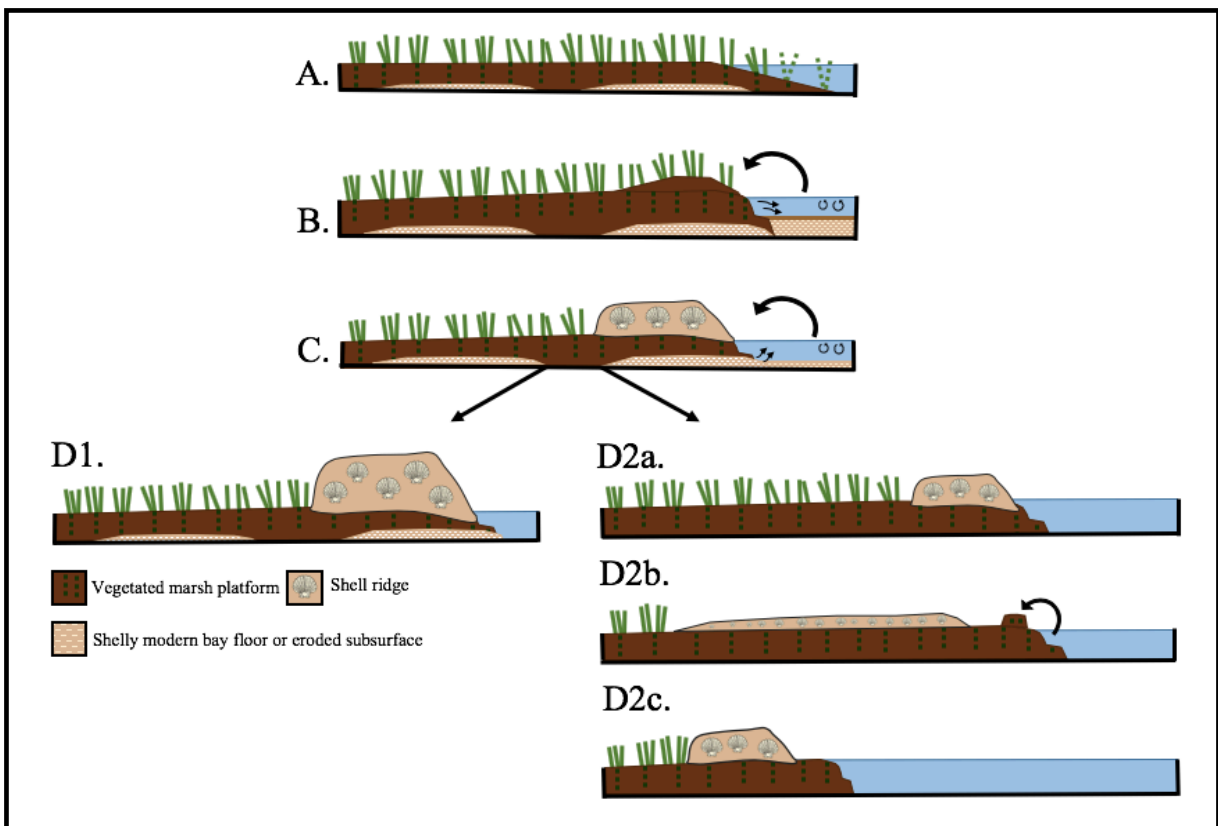


Figure 19: Conceptual model of shell ridge development with modified steps from models developed by Ellison (2011) and Wilson and Allison (2008). (A) Slowly subsiding marsh. (B) Erosional scarp formed on marsh edge. Material becomes suspended and placed on marsh surface with high wave and tide action. (C) Eventually, large shell pieces are also placed on shore during stronger energy events (i.e. storms) from either the modern bay floor or eroded subsurface. (D1) Shell ridge is high, leading to its stability and marsh vegetation behind the ridge remains. (D2a and D2b) Shell ridge is shorter, leading to its translation inland. This mobile ridge spreads out across the marsh platform and subsequently exposes a platform without aboveground vegetation, but still contains belowground biomass. “Blocks” of marsh edge can be transported onshore from wave action. (D2c) The marsh platform now lacks of aboveground vegetation to dampen wave energy (Méndez et al., 1999), leading the shells to reaccumulate.

The separation better illustrates what exactly happens to the shell ridges and the marsh vegetation as the shell ridges either remain stable or spread across the marsh and eventually reconsolidate again with wave action.

4.2 Shell ridge movement

4.2.1 Effect of storm surge and wind direction

Winter cold fronts and tropical cyclones are both capable of producing water level set up and wave energy that can overtop Louisiana marsh platforms (Reed, 1989b; Dietrich, 2011). During a two-year study Thomason (2016) concluded that most movement of shell ridges in a nearby study area occurred during and immediately following an extratropical cyclone event. In the course of this investigation, there were cold fronts and cyclone activity that could have affected the Biloxi Marsh.

The largest storm to affect the study area during the July-January span of this project was Hurricane Nate, which made landfall near the mouth of the Mississippi River on 10/7/17 around 7:00 p.m. CT as a Category 1. This event occurred during the approximately 1-month period in between sampling the sites on 9/13/17 and 10/11/17 and coincides with the largest shell ridge cross-marsh translation measured at five of nine ridges. Movement during this timeframe was as much as 20.63 m inland and the ridges that showed the most movement during this period were located on the north and south side of the island.

4.2.2 Effect of individual ridge characteristics, fetch conditions, and wind direction

Ridge mobility at various study sites was most dependent upon how exposed that ridge was to large fetch conditions (Fig. 7). All four of the mobile ridges (1, 4, 5, 8) were located along areas of the island where fetch, hence wave energy, could have contributed significantly toward progressive landward movement. Five of the nine ridges, however, remained relatively stable.

These included ridges 2, 3, 6, 7, and 9. Ridge 2 contained two smaller shell accumulations that were open to significant fetch conditions, however, immediately behind the ridges was a small channel in the marsh. Field observations found that the shells were being deposited into this small channel, preventing the migration of shell ridges beyond it. Ridge 3 was located along the large interior channel separating the two large islands, which protected the ridge from wave energy. Ridge 6 overlies the area of the island that is relatively more vertically stable above an old distributary channel. Ridge 6 was also the tallest and one of the widest of the examined ridges, with a maximum width of 26.80 m and maximum relief of 1.53 m. This suggests that it is more difficult for large waves to be able to move significant quantities of shell that could otherwise be moved in more narrow, and lower ridges. Ridge 7 was also located on the island segment that overlies a paleo distributary channel. This might be the only reason to explain its stability, as the ridge was otherwise lower and more narrow, exposed to a relatively large fetch, and consequently would be expected to be more mobile, however it was not. Ridge 9 was also designated as a stable ridge and its geomorphic behavior is likely due to its location on a relatively fetch protected segment of the islands, near the mouth of the interior channel that separates the two islands.

There does appear to be some correlation with primary wind direction during certain time periods and the highest amounts of movement with ridges exposed to that wind direction (correlations occurred with both stable and mobile ridges). From 7/26/17 to 9/13/17, the highest amount of movement at Ridge 9 occurred. Ridge 9 was exposed to the north and the dominant wind direction was north as well. From 9/13/17 to 10/11/17, five of the nine sites (Ridges 1, 2, 4, 5, and 8) showed their highest amounts of movement and these ridges were exposed to the dominant wind direction of that period (NE-ENE or S-SSE).

Finally, there was no evident pattern of stable or mobile ridges having relatively more or less likelihood to fragment. For example, half of the six ridges that showed any sort of fragmentation were stable ridges and half were mobile ridges. Therefore, fragmentation provides no insight to the whether a ridge is stable or mobile, but may just be a function of original formation conditions.

4.3 Shell ridge effect on marsh

The above- and belowground biomass results indicate that shell ridges do have a lasting effect on the marsh, particularly on the aboveground biomass. Keeping in mind that the large presence of dead biomass over alive biomass site-wide is most likely attributed to the data being collected in winter (2/1/18) and early spring (4/2/18), the highest averages of total biomass above- and belowground were found at sites where no shell ridge was present. Locations such as these represent unaltered marsh platform that has not be affected by the transfer of shells to the marsh platform. However, the biomass production was still affected by interior ponding and shoreline erosion, as shown by the extremely low amounts of biomass along the shorelines and in the interior marsh where interior ponding was noted.

When ridges are stable, aboveground biomass measurements are some of the highest values behind the ridge, with a 14% increase for dead biomass and a 226% increase for alive biomass. This suggests that the marsh behind the stable ridges at these sites is less affected by wave energy than at other sites. However, at Ridge 6, where shells were able to be dug up in the middle of the stable shell ridge and plots placed, there was no vegetation present, indicating that while stable ridges move less and affect less vegetation behind it, it has clearly damaged the aboveground vegetation that was present underneath.

At sites where ridges were mobile, there was a stark lack of aboveground vegetation in front of the shell ridges. The consequence of this lack of aboveground vegetation is that there is nothing present to dampen wave energy (Méndez et al., 1999; Méndez and Losada, 2004). The marsh platform in front, below, and behind mobile ridges is still heavily vegetated belowground, and along the marsh edge, it was evident from field observations that the terraced scarps break apart into “blocks” of marsh and are placed onto the edge of the marsh platform (Fig. 20). No other example of this feature was found in literature, however, it is believed this is a result of wave attack along the marsh scarp and should be studied in the future. Additionally, while erosion is likely in front of these mobile shell ridges, behind the shell ridge, the vegetation is still relatively abundant. This is reasonable, as the shells have not yet superimposed on the vegetation, causing it to smother.

Statistical analysis shows that above- and belowground biomass at all sites with the exception of one, is not statistically significant. This suggests that while there are differences in the means (Fig. 15), they are not statistically significant. For instance, an aboveground comparison between sites without a ridge and with a mobile ridge shows significant differences ($p=0.03$) suggesting that ridge mobility does affect aboveground biomass. However, aboveground biomass for sites without a ridge and with a stable ridge, show no significant differences ($p=0.81$), suggesting that marshes behind the stable ridge fair similarly to sites without a ridge and are perhaps not negatively affected by the ridge, but as expected marshes immediately below the ridge likely are negatively affected. The statistical test, however, did not show this response likely because of lack of access to some locations and a low number of observations ($n=6$ or $n=8$). Another issue that may contribute to somewhat inconclusive statistical testing is the grouping of the dead and live biomass. Nonetheless, some of the

comparisons are close (i.e. $p \sim 0.1$) to being significant ($p \sim 0.05$) and would be more conclusive if more samples were available.

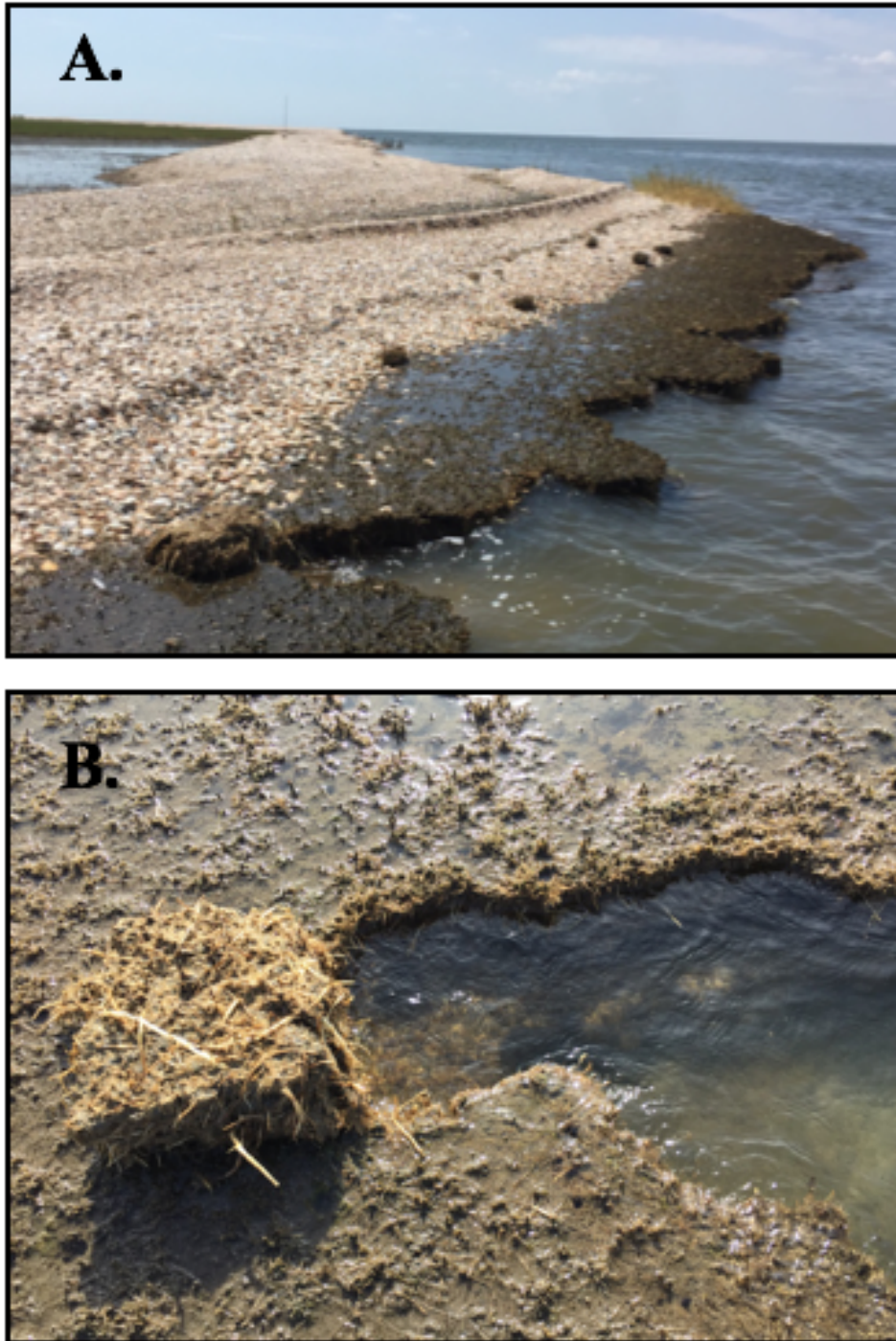


Figure 20: Ridge 7 on 1/10/18. (A) “Blocks” of marsh platform scattered onshore from eroded marsh scarp. (B) Up close image of “block” of marsh platform next to terraced marsh scarp where it likely eroded from.

4.3.1 Future work

Future studies on the effect of shell ridges on marsh platforms should analyze interior ponding patterns and regrowth of vegetation after a shell ridge moved into the interior marsh, leaving an unvegetated marsh platform. While interior ponding was discussed at both sites without a shell ridge and with a stable ridge, it was also seen at sites with a mobile shell ridge and a possible correlation with increased interior ponding at certain ridge types should be studied. It could be hypothesized that when large scale flooding events occur, water would be unable to drain from behind stable shell ridges, leading to increased waterlogging of the vegetation, which has shown to cause dieback amongst *Spartina alterniflora* (Mendelssohn and Seneca, 1980; Mendelssohn and McKee, 1988). As for regrowth of vegetation once a shell ridge has moved into the interior marsh, a study that analyzed hurricane overwash effects on vegetation found that *Spartina alterniflora* could regrow in “islands” from a combination of regrowth of buried plants and seed recruitment from nearby surviving species (Courtemanche et al., 1999). However, the amount of time vegetation is covered by shell ridges and distances between unvegetated platforms and surviving species both vary greatly and could make the case very different for shell ridge overwash.

4.4 Future of Biloxi Marsh due to shell presence

Satellite imagery suggests that periods of accumulation and overwash of shell ridges, as well as shoreline retreat and shell ridge reaccumulation have been occurring for at least the last few decades. Imagery also reveals that the side of the island that has shell ridges (western side) retained a consistent shape through time and showed significantly less shoreline retreat compared to the side of the island that does not have shell ridges (eastern side), which more often showed more significant shoreline erosion. This information, in addition to the results of the modern

shell ridges studied here, shows that shell ridges in the past and present are dictating the morphology of the Biloxi Marsh and are likely to continue to do so in the future.

It can be expected that in the future these marshes will remain more stable where ridges are stable because wave and tide energy does not reach the interior marsh and shell material is not as likely to overwash onto the marsh, causing the vegetation to smother and die. However, marshes will likely erode where ridges are mobile (even more than sites without any shell ridges) because of the subsequent exposed and denuded marsh platform that is left more susceptible to erosion.

Eventually, it can be expected that with the rise in sea level and ever consistent storm conditions (Day and Templet, 1989; Mariotti et al., 2010) that these marshes will erode away nonetheless, leaving shells accumulated at the surface and eventually becoming submerged as a subaqueous shell mound as predicted by Ellison (2011).

CHAPTER 5. CONCLUSION

An understanding of all the processes that cause coastal erosion and shape the modern landscape of coastal Louisiana is critical to the effort of minimizing and mitigating against the widespread land loss of the region. One previously unstudied contributor to marsh dieback and ultimately erosion is the accumulation of shell ridges along the edges of marsh platforms of the Biloxi Marsh. This study shows that:

1) There exists substantial variation in the source of shells. Most of the shell ridges examined consisted of predominantly *Crassostrea virginica*, which were relatively young in age, less than 1.0 ky. This points to nearby man-made oyster fisheries or natural oyster reefs as probable sources. The second most common species was *Rangia cuneata* shells, which are older and likely being excavated from subsurface St. Bernard delta deposits.

2) Shell ridges are stable in areas that are exposed to less fetch, when they are relatively large, or when they overlie marshes with underlying stable strata. Shell ridges are mobile in locations that are exposed to relatively larger fetch.

3) Vegetation that grows behind stable shell ridges is robust, whereas vegetation that grows behind mobile ridges is eventually smothered by translation of shells onto the marsh platform. This leaves a platform denuded of surface vegetation, but heavily rooted belowground. The lack of significant aboveground vegetation allows waves to wash farther onto the platform with no vegetation to dampen the energy (Méndez et al., 1999; Méndez and Losada, 2004), while a still heavily vegetated marsh platform with scarped terraces at its edge breaks into “blocks” that are deposited onshore.

4) In the future, marshes will remain more stable where shell ridges are stable because the interior marsh is not affected by wave and tide energy and shell material is not as likely to

overwash onto the marsh and smother the vegetation. However, marshes will likely erode where shell ridges are mobile because of the subsequent exposed and denuded marsh platform that is left more susceptible to erosion. It is predicted that eventually, with the rise in sea level and persistent storm conditions (Day and Templet, 1989; Mariotti et al., 2010), these marshes will inevitably erode away, leaving shell accumulations that were first deposited at the surface but eventually becoming submerged as a subaqueous shell mound.

References

- Alexander, C., 2008. Rates of Processes of Shoreline Change at Ft. Pulaski National Monument. Final Report. Applied Coastal Research Laboratory. Statesboro, GA. 1-58.
- Allen, J.R.L., 1984. Experiments on the settling, overturning and entrainment of bivalve shells and related models. *Sedimentology*, 31, 227-250.
- Augustinus, P.G.E.F., 1980. Actual development of the chenier coast of Suriname (South America). *Sedimentary Geology*. 26(1-3). 91-113.
- Byrne, J.V., Leroy, D.O.S., and Riley, C.M., 1959. The chenier plain and its stratigraphy, southwestern Louisiana. *Gulf Coast Association of Geological Societies Transactions*. 9, 237-260.
- Courtemanche Jr., R.P., Hester, M.W., and Mendelssohn, I.A., 1999. Recovery of a Louisiana Barrier Island Marsh Plant Community following Extensive Hurricane-Induced Overwash. *Journal of Coastal Research*, 15(4), 872-883.
- Couvillion, B., Barras, J., Steyer, G., Sleavin, W., Fischer, M., Beck, H., Trahan, N., Griffin, B., & Heckman, D., 2011. Land area change in coastal Louisiana (1932-2010). U.S. Geological Survey Scientific Investigations Map 3164, scale 1:265,000, 12 p. pamphlet.
- Darby, F., 2006. Belowground biomass of *Spartina alterniflora*: seasonal variability and response to nutrients. *LSU Doctoral Dissertations*. 1-99.
- Day Jr., J.W., Britsch, L.D., Hawes, S.R., Shaffer, G.P., Reed, D.J. and Cahoon, D., 2000. Pattern and process of land loss in the Mississippi Delta: a spatial and temporal analysis of wetland habitat change. *Estuaries*, 23(4), 425-438.
- Day Jr., J.W. and Templet, P.H., 1989. Consequences of sea level rise: implications from the Mississippi Delta. *Coastal Management*, 17(3), 241-257.
- Dietrich, J.C., Westerink, J.J., Kennedy, A.B., Smith, J.M., Jensen, R.E., Zijlema, M., Holthuijsen, L.H., Dawson, C.N., Luettich, R.A. Jr., Powell, M.D., Cardone, V.J., Cox, A.T., Stone, G.W., Pourtaheri, H., Hope, M.E., Tanaka, S., Westerink, L.G., Westerink, H.J., Cobell, Z., 2011. Hurricane Gustav (2008) waves, storm surge and currents: hindcast and synoptic analysis in Southern Louisiana. *Monthly Weather Review*. 139(8), 2488-2522.
- Dunbar, J.B., Blaes, M.R., Dueitt, S.E., May, J.R., Stroud, K.W., 1994. Geological investigation of the Mississippi River deltaic plain. Report 2, Technical Report GL-84-15, prepared for U.S. Army Corps of Engineers, New Orleans.
- Ellison, M., 2011. Subsurface controls on mainland marsh shoreline response during barrier island transgressive submergence. *University of New Orleans Theses and Dissertations*. 1-133.
- Fearnley, S., Penland, S. and Britsch, L.D., 2009. Mapping the geomorphology and processes of coastal land loss in the Pontchartrain Basin: 1932 to 1990 and 1990 to 2001. *Journal of Coastal Research*, 48-58.
- Fisk, H.N., 1955. Sand facies of recent Mississippi Delta deposits. *World Petroleum Congress*. 379-398.
- Frazier, D., 1967. Recent deltaic deposits of the Mississippi River: Their development and chronology. *Gulf Coast Association of Geological Societies Transactions*. 17. 287-315.

- Gallagher, J. L., 1974. Sampling Macro-Organic Matter Profiles in Salt Marsh Plant Root Zones. *Soil Science Society of America Journal*. 38, 54-155.
- Gedan, K.B., Kirwan, M.L., Wolanski, E., Barbier, E.B., Silliman, B.R., 2011. The present and future role of coastal wetland vegetation in protecting shorelines: answering recent challenges to the paradigm. *Climatic Change*, 106, 7-29.
- Gould, H.R. and McFarlan, E., 1959. Geologic history of the chenier plain, southwestern Louisiana. *Gulf Coast Association of Geological Societies Transactions*. 9, 261-272.
- Hoyt, J.H., 1969. Chenier versus barrier, genetic and stratigraphic distinction. *Bulletin of American Association of Petroleum Geologists.*, 53(2), 299-306.
- Kesel, R.H., 1988. The decline in the suspended load of the lower Mississippi River and its influence on adjacent wetlands. *Environmental Geology and Water Sciences*, 11, 271-281.
- Kindinger, J.L., 1988. Seismic stratigraphy of the Mississippi-Alabama shelf and upper continental slope. *Marine Geology*. 83(1-4). 79-94.
- Kolb, C.R., and van Lopik, J.R., 1958. Geological Investigation of the Mississippi River-Gulf Outlet Channel: U.S. Army Corps of Engineers, Waterways Experiment Station, Miscellaneous Paper 30259, Vicksburg, Mississippi.
- Kolb, C. R. and Van Lopik, J.R., 1958. Geology of the Mississippi Deltaic Plain—Southeastern Louisiana. U.S. Army Engineers Waterways Experiment Station, Technical Report 2:3-482. Vicksburg, Mississippi.
- Liu, C., & Walker, H., 1989. Sedimentary characteristics of cheniers and the formation of the chenier plains of East China. *Journal of Coastal Research*, 5(2), 353-368.
- Mariotti, G., Fagherazzi, S., Wiberg, P.L., McGlathery, K.J., Carniello, L. and Defina, A., 2010. Influence of storm surges and sea level on shallow tidal basin erosive processes. *Journal of Geophysical Research: Oceans*, 115(C11012). 1-17.
- Meade, R.H. and Moody, J.A., 2010. Causes for the decline of suspended-sediment discharge in the Mississippi River system, 1940–2007. *Hydrological Processes*, 24(1), 35-49.
- Mendelssohn, I.A. and Seneca, E.D., 1980. The influence of soil drainage on the growth of salt marsh cordgrass *Spartina alterniflora* in North Carolina. *Estuarine and Coastal Marine Science*, 11(1), 27-40.
- Mendelssohn, I.A. and McKee, K.L., 1988. *Spartina alterniflora* die-back in Louisiana: time course investigations of soil waterlogging effects. *Journal of Ecology*, 76(2), 509-521.
- Méndez, F.J. and Losada, I.J., 2004. An empirical model to estimate the propagation of random breaking and nonbreaking waves over vegetation fields. *Coastal Engineering*, 51(2), 103-118.
- Méndez, F.J., Losada, I.J., Losada, M., 1999. Hydrodynamics induced by wind waves in a vegetation field. *Journal of Geophysical Research*. 104(C8). 18,383-18,396.
- Neal, A., Richards, J., Pye, K., 2002. Structure and development of shell cheniers in Essex, southeast England, investigated using high-frequency ground-penetrating radar. *Marine Geology*, 185(3-4), 435-469.

- Otvos, E., 2000. Beach ridges – definitions and significance. *Geomorphology*, 32(1-2), 83-108.
- Otvos, E., Price, A., 1979. Problems of chenier genesis and terminology – an overview. *Marine Geology*, 31(3-4), 251-263.
- Penland, S., Boyd, R. and Suter, J.R., 1988. Transgressive depositional systems of the Mississippi delta plain: a model for barrier shoreline and shelf sand development. *Journal of Sedimentary Research*, 58(6), 932-949.
- Penland, S., Beall, A.D., Britsch, L.D. III, Williams, S.J., 2002. Geologic classification of coastal land loss between 1932 and 1990 in the Mississippi River Delta Plain, Southeastern Louisiana. *Gulf Coast Association of Geological Societies Transactions*, 52, 799-807.
- Poirrier, M., Rodriguez del Rey, Z., Spalding, E., 2008. Acute disturbance of Lake Pontchartrain benthic communities by Hurricane Katrina. *Estuaries and Coasts*, 31(6), 1221-1228.
- Reed, D., 1989a. The role of salt marsh erosion in barrier island evolution and deterioration in coastal Louisiana. *Transactions - Gulf Coast Association of Geological Societies*, 39, 501-510.
- Reed, D., 1989b. Patterns of Sediment Deposition in Subsiding Coastal Salt Marshes, Terrebonne Bay, Louisiana: The Role of Winter Storms. *Estuaries*, 12(4), 222-227.
- Reineck H.E., Singh, I.B., 1980. Depositional Sedimentary Environments. Springer-Verlag Berlin Heidelberg New York. 354-355.
- Rhodes, E., 1980. *Modes of Holocene coastal progradation: Gulf of Carpentaria*. Thesis (Ph.D.) Australian National University.
- Roberts, H., 1997. Dynamic changes of the Holocene Mississippi River Delta Plain: The delta cycle. *Journal of Coastal Research*, 13(3), 605–627.
- Rodriguez-Ramirez, A., Yáñez-Camacho C.M., 2008. Formation of chenier plain of the Doñana marshland (SW Spain): observations and geomorphic model. *Marine Geology*, 254, 187–196.
- Rogers, B.E., Kulp, M.A. and Miner, M.D., 2009. Late Holocene chronology, origin, and evolution of the St. Bernard Shoals, northern Gulf of Mexico, USA. *Geo-Marine Letters*, 29(6), 379-394.
- Russell, R., & Howe, H., 1935. Cheniers of Southwestern Louisiana. *Geographical Review*, 25(3), 449-461.
- Schubauer, J.P. and Hopkinson, C.S., 1984. Above-and belowground emergent macrophyte production and turnover in a coastal marsh ecosystem, Georgia. *Limnology and Oceanography*, 29(5), 1052-1065.
- Shumway, S.E., 1996. Natural environmental factors. In: Kennedy, V.S., Newell, R.I.E., Eble, A.F. (Eds.), *The Eastern Oyster Crassostrea virginica*. Maryland Sea Grant College, University of Maryland System, College Park, 185–223.
- Thomason, R., 2016. Biloxi Marsh Platform Response due to Meteorological Forcing. *University of New Orleans Theses and Dissertations*. 1-103.

- Tonelli, M., Fagherazzi, S., & Petti, M. (2010). Modeling wave impact on salt marsh boundaries. *Journal of Geophysical Research: Oceans* (1978–2012), 115(C9).
- Törnqvist, T.E., Kidder, T.R., Autin, W.J., van der Borg, K., de Jong, A.F., Klerks, C.J., Snijders, E.M., Storms, J.E., van Dam, R.L. and Wiemann, M.C., 1996. A revised chronology for Mississippi River subdeltas. *Science*, 273(5282), 1693-1696.
- Törnqvist, T.E., Wallace, D.J. Storms, J.E.A., Wallinga, J., Van Dam, R.L., Blaauw, M., Derksen, M.S., Klerks, C.J.W., Meijneken, C., Snijders, E.M.A., 2008. Mississippi Delta subsidence primarily caused by compaction of Holocene strata. *Nature Geoscience*, 1(3), 173-176.
- Törnqvist, T.E., Rosenheim, B.E., Hu, P., Fernandez, A.B., 2015. Radiocarbon dating and calibration. In: Shennan, I., Long, A.J., Horton, B.P. (Eds.), *Handbook of Sea-Level Research*. Wiley, 349-360.
- Trosclair, K.J., 2013. Wave transformation at a saltmarsh edge and resulting marsh edge erosion: observations and modeling. 1-73.
- Tunnell Jr., J.W., Andrews, J., Barrera, N.C., Moretzsohn, F., 2010. *Encyclopedia of Texas Seashells*. Texas A&M University Press, College Station, TX
- Weill, P., Mouazé, D., Tessier, B. and Brun-Cottan, J.C., 2010. Hydrodynamic behaviour of coarse bioclastic sand from shelly cheniers. *Earth Surface Processes and Landforms*, 35(14), 1642-1654.
- Wilson, C.A. and Allison, M.A., 2008. An equilibrium profile model for retreating marsh shorelines in southeast Louisiana. *Estuarine, Coastal and Shelf Science*, 80(4), 483-494.

Appendix

Ridge	Movement (m)					Stable or Mobile	Fragmentation	Fetch (km)
	From 7/26/17 to 9/13/17	From 9/13/17 to 10/11/17	From 10/11/17 to 1/10/18	Total From 7/26/17 to 10/11/18	Total From 7/26/17 to 1/10/18			
	1	4.63	5.62	0.04	10.25			
2a	0.5	3.89		4.39		Stable	Major Increase	46.38
2b	2.17	2.32		4.49		Stable		46.71
3	-0.41	-0.14		-0.55		Stable	Remained Fragmented	0.09
4	0.99	5.94		6.93		Mobile	Major Increase	41.7
5	2.2	10.97	-0.09	13.17	13.08	Mobile	Major Increase	41.61
6	2.28	2.4	4.39	4.68	9.07	Stable	Remained Whole	1.54
7	1.53	1.89	5.6	3.42	9.02	Stable	Minor Increase	1.57
8	20.13	20.63	-2.82	40.76	37.94	Mobile	Remained Fragmented	21.18
9	2.31	0.87		3.18		Stable	Major Increase	0.27

Table 1: Magnitude of shell ridge translation from 7/26/17 to 10/11/17 or 1/10/18 (only five sites were measured on 1/10/18). The magnitude of movement during this ~2.5 month time period was the basis for determining whether a ridge was mobile or stable, wherein all movement less than 5 m were considered stable and movement more than 5 m was considered mobile. In addition to whether a ridge was mobile or stable, the amount of shell fragmentation and open fetch at each of the shell ridges during the study period are listed.

Ridge	Width (m)					Tallest Height along Transect (m)				
	7/26/18	9/13/18	10/11/18	1/10/18	% Increase	7/26/18	9/13/18	10/11/18	1/10/18	% Increase
	1	11.1	9.78	11.02	11.52	3.78	0.84	0.97	0.57	0.57
2a	8.72	8.39	8.81		1.03	0.56	0.57	0.44		-21.19
2b										
3	4.78	4.44	4.89		2.30	0.73	0.73	0.61		-15.95
4	16.27	18.01	24.62		51.32	0.76	0.78	0.65		-13.54
5	13.33	10.55	18.84	18.93	42.01	0.64	0.61	0.51	0.53	-18.12
6	22.27	21.89	22.16	17.87 21.31 28.06*	26	1.53	1.26	0.95	1.37 1.13 0.92*	-40.20
7	4.26	5.27	14.18	9.73	128.40	0.72	0.74	0.53	0.61	-14.97
8										
9	8.73	5.99	8.33		-4.58	0.62	0.64	0.34		-45.78

Table 2: Widths and heights of shell ridges from 7/26/18 to 10/11/17 or 1/10/18 (only four sites had widths and heights measured on 1/10/18) as well as their corresponding percent increases. Note that Ridge 6 is broken up into three width and height measurements and that stars (*) note which measurements on 1/10/18 are used for percent increase.

Ridge	Area (m ²)					Volume (m ³)				
	7/26/18	9/13/18	10/11/18	1/10/18	% Increase	7/26/18	9/13/18	10/11/18	1/10/18	% Increase
1	405.53	371.44	402.05	631.62	55.75	706.62	650.48	554.82	610.46	-13.61
2a	54.26	48.48	63.16		16.41	50.65	51.65	42.37		-16.35
2b	55.55	50.39	76.35							
3	302.41	207.33	203.22		-32.80	490.41	272.56	232.05		-52.68
4	1153.95	1218.23	2081.25		80.36	2064.62	2334.53	4044.01		95.87
5	1280.71	1291.85	1334.98	1628.78	27.18	1791.67	932.94	1143.47	1412.83	-21.14
6	2098.92	2046.76	2438.55	1715.96	-18.25	6740.06	8418.80	7184.20	3636.10	-46.05
7	663.83	544.59	1067.14	589.01	-11.27	366.04	404.19	995.99	579.20	58.23
8	743.84	544.06	820.64	915.32						
9	391.22	303.92	644.28		64.69	464.56	323.81	147.47		-68.25

Table 3: Areas and volumes of shell ridges from 7/26/18 to 10/11/17 or 1/10/18 (only five sites had widths and heights measured on 1/10/18) as well as their corresponding percent increases.

VITA

The author was born in New Orleans, Louisiana and raised in Lafayette, Louisiana and Pensacola, Florida. She obtained her undergraduate degree from Louisiana State University in Geology and Geophysics, where she focused her studies on deltaic sedimentology and stratigraphy, graduating in the spring of 2016. The following August, she enrolled at the University of New Orleans to earn her Master's degree, focusing her studies on coastal geomorphology.